Progression Report

Climate Impacts of the Intensification of Northern Hemisphere Glaciation

Friso de Graaf

School of Geography,
Queen Mary University of London

Supervisors:

Dr. Heather L. Ford (QMUL Geography)
Prof. David Thornalley (UCL Geography)
Dr. Anna Bourne (QMUL Geography)
Dr. David Wilson (UCL Earth Sciences)

December 2022

Contents

1 Introduction

1.1 Background

The intensification of Northern Hemisphere Glaciation (iNHG) is a major reorganisation of the Earth's climate and one of the largest secular changes in the last 5 million years (Driscoll and Haug, 1998; Bartoli et al., 2005). The iNHG begun at the end of the Pliocene, roughly 2.7 million years ago (Ma), with the growth of large ice sheets across North America, Europe and Asia. The Pliocene was followed by the Pleistocene, characterised by the advance and retreat of ice sheets across the Northern Hemisphere, causing hundred-metre fluctuations in sea levels and marked climate changes. Permanent ice sheets were established on Greenland and West Antarctica over the iNHG, and atmospheric temperatures cooled considerably; 3 - 4°C in the tropics, over 10°C at the poles (Raymo, 1994). These changes also had a major impact on the internal structure of the world's oceans.

In the modern day, water in the deep oceans (below c. 3000 m depth) is produced by sinking water masses at high latitudes in the North Atlantic and Southern Oceans (Talley, 2013). These water masses sink to depth, fill the deep oceans, and then upwell and recirculate. Deep waters formed in the North Atlantic upwell in the Southern Ocean, combine with surface waters and return to the North Atlantic, forming the Atlantic Meridional Overturning Circulation (AMOC) cell (Talley et al., 2011). Despite similarly cold temperatures, deep waters are not formed in the modern North Pacific Ocean due to the presence of a strong salinity gradient, or halocline (Warren, 1983). The fresh surface waters of the subpolar North Pacific have a buoyancy that inhibits deep water formation. The deep Pacific Ocean is therefore filled with Antarctica Bottom Waters (AABW) and Circumpolar Deep Waters (CDW) from the Southern Ocean (Talley, 2013).

Climate modelling results suggest that the North Pacific halocline was eroded in the Pliocene allowing for the formation of North Pacific Deep Waters (NPDW) and creating a Pacific Meridional Overturning Circulation (PMOC) cell (Burls et al., 2017). This PMOC may have resulted from the reduced meridional sea surface temperature (SST) gradients and weaker atmospheric moisture transport in the Pliocene Pacific Ocean relative to today (Burls et al., 2017). The evidence for deep water formation in the subpolar North Pacific is absent in the Early Pleistocene (Swann, 2010), suggesting that the PMOC is halted over the iNHG (Burls et al., 2017). This is most likely due to the establishment of a strong North Pacific halocline, but how and when this process occurred is poorly understood. The characteristics of the deep Pacific Ocean converge with those of the deep Atlantic over the iNHG (Woodard et al., 2014), suggesting increased connectivity between the Atlantic and Pacific after the iNHG.

1.1.1 The AMOC

The strength of the AMOC over the iNHG is also uncertain, with contradictory evidence of both AMOC strengthening (Hayashi et al., 2020) and weakening (Lang et al., 2016) over the iNHG. Determining the change in AMOC strength is complicated by uncertainties over AMOC strength prior to the iNHG, in the Late Pliocene. A PMOC during the Late Pliocene may have weakened the AMOC in the Atlantic (Ferreira et al., 2018), while climate modelling evidence suggests that AMOC strength remained similar to the modern in the Pliocene (Zhang et al., 2013). A strong AMOC would result in NADW export out of the Atlantic Ocean and could be responsible for the convergence in deep water mass properties between the Atlantic and Pacific Oceans over the iNHG (Kwiek and Ravelo, 1999; Woodard et al., 2014).

1.1.2 Impact of iNHG on Volcanism

The iNHG is defined by the growth of major ice sheets across the Northern Hemisphere, and this expansion may have changed rates of volcanism on Iceland. Given the importance of volcanism in regulating the climate (McKenzie et al., 2016), this changes in volcanism over the iNHG could have had wide-reaching climatic effects. At the end of the last glacial periods there is evidence for a marked increase in volcanism on Iceland as ice sheet retreated, reducing the ice loading on the crust and allowing more magma to rise to the surface and melt (Maclennan et al., 2002). The iNHG would have caused rapid changes in the ice loading on Iceland as ice sheets advanced and retreated in the Early Pleistocene, which would have had an impact on the rates of volcanism on the island.

1.2 Proposed Chapters, Knowledge Gaps and Aims

The three chapters of this project will look at changes in: ocean structure in the Pacific, AMOC strength, and the rates of volcanism on Iceland in response to the iNHG.

1.2.1 Ocean Structure in the Pacific

The first chapter looks at ocean circulation in the Pacific over the iNHG. The circulation in the deep Pacific Ocean was likely different during the Pliocene compared to the present, as shown by the palaeo-proxy evidence from a PMOC (Burls et al., 2017; Shankle et al., 2021; Ford et al., 2022). However, a PMOC is not simulated in most climate models (Tan et al., 2020; Zhang et al., 2021) which suggest that the mechanism for formation of an overturning cell in the Pacific is not full understood. The timing and nature of the cessation of the PMOC over the iNHG is not currently well resolved, and better constraining this process could shed light on the mechanism driving the basin-wide circulation.

There is evidence that points to a greater connectivity between the Atlantic and Pacific Oceans after the iNHG, with more heat and salt transport between the two basins (Woodard et al., 2014). This increase in connectivity may be related to the shutdown of the PMOC over the iNHG or could be driven by changes in the Southern Ocean.

The aims of this first chapter are therefore:

1. To characterise the temperature, carbon storage, and salinity of deep waters in the North Pacific.

2. To understand how these properties change over the iNHG.

3. To determine how the cessation of the PMOC fits in to the wider climate changes occurring over the iNHG.

1.2.2 Changes in AMOC Strength

The second chapter seeks to look at how the strength of the AMOC changed over the iNHG. There is contradictory evidence pointing to a stronger (Hayashi et al., 2020), weaker (Lang et al., 2016), and similar strength (Hodell and Venz, 1992) AMOC to the present over the iNHG. The weaker AMOC signal after the iNHG may be the result of aliasing issues where weaker circulation during glacial periods of the Early Pleistocene decreases the average strength of Atlantic circulation (Raymo et al., 1992). AMOC strength is largely inferred from the spatial extent of North Atlantic Deep Water (NADW), with a larger extent implying stronger overturning (Hodell and Venz, 1992; Raymo et al., 1992; Lang et al., 2016). However, modelling and palaeoenvironmental evidence suggest greater deep water formation in the Southern Ocean during the Late Pliocene (Hill et al., 2017; McKay et al., 2012), which would reduce the extent of northern-sourced deep waters without any change in overturning circulation strength.

The relative strength of deep-water export from the North Atlantic and Southern Ocean can be seen in the spatial extent of northern- and southern-sourced water masses in the deep mid-Atlantic Ocean. The characteristics of NADW and AABW are poorly defined over the iNHG in terms of temperature, salinity, and carbon storage. A clearer understanding of these properties could help to constrain past ocean circulation.

The aims of this chapter are:

1. To describe the temperature, salinity, and carbon content of NADW and AABW water masses before and after the iNHG.

2. To determine the relative influence of northern- and southern-sourced waters on the deep mid-Atlantic before and after the iNHG.

3. To determine how AMOC strength changed over the iNHG and the role this may have played in wider oceanographic changes.

1.2.3 Impact on Volcanism

The final chapter looks at the impacts that the iNHG may have had on volcanism. The iNHG likely caused a change in the rate of volcanism due to the loading of major ice sheets over areas such as Iceland. The impact of this process is poorly understood due to the limited number of records of volcanism from the Late Pliocene and Early Pleistocene. Tephra records from the Holocene and Late Pleistocene have shown that there are statistically significant changes in the rate of volcanism due to ice loading

(Maclennan et al., 2002; Sigmundsson et al., 2010, 2012). It is expected that there will be similar changes observed over the iNHG.

The aims of this final chapter are:

1. To construct a record of volcanism on Iceland for the Late Pliocene and Early Pleistocene from tephra in marine sediments cores.

2. To determine if there is a significant change in the rate of volcanism over the iNHG on Iceland.

1.3 Signficance

The iNHG represents a uniquely accessible natural experiment of how the Earth's climate responds to major climatic changes. The PMOC is a good example of the limits of climate models in explaining the behaviour of the climate in response to secular changes. As the world warms due to the effects of anthropogenic warming, it is increasingly important to understand the dynamics of ocean circulation and how they are influenced by rapid temperature changes.

The Pacific Ocean is a major store of carbon and heat in the modern oceans (Cheng et al., 2017). Changing the ventilation of the deep Pacific Ocean would have major impacts on the carbon balance, markedly increasing the amount of CO_2 in the atmosphere, as well as releasing heat that has been stored in the deep ocean. The deep oceans are also major stores of nutrients, the upwelling of which can profoundly impact coastal communities. The circulation of the deep Atlantic and Pacific Oceans therefore has major economic and ecological impacts. This project seeks to further our understanding of the deep circulation of these oceans, and how the deep sea carbon storage may have changed in the past.

Volcanism as well as the deep oceans can have large impacts on the climate in the short term (Rampino and Self, 1993). The interplay between volcanism and the climate on longer timescales is less well understood. This project would seek to address this, and therefore improve our knowledge of how the Earth works and how fundamental forces such as plate tectonics and the climate interact.

1.4 Report Structure

This report will undertake a thorough review on the existing literature on the topics mentioned in the introduction and then outline the path of the PhD project in addressing the aims mentioned above. The literature review is structured in two parts, the first dealing with oceanography and the second with volcanism.

The oceanography section of the literature review begins by describing the changes that occurred over the iNHG and how well we can constrain the nature and timings of these events. Then it covers the modern structure of the Pacific, Atlantic and Southern Oceans. This is followed by a discussion of the Atlantic and Pacific Oceans over the Late Pliocene and the iNHG, focussing in particular on:

1. The controversy over the extent of overturning circulation in the Late Pliocene Pacific Ocean.

2. The possible explanations for the declining PMOC strength over the iNHG.

3. The competing evidence for changes in AMOC strength over the iNHG.

4. The reasons why we see a convergence in deep water mass properties in the Atlantic and Pacific Oceans over the iNHG.

The final part of this section will cover the techniques that will be used to answer these questions: oxygen isotopes, Mg/Ca, B/Ca and $\varepsilon_{\mathrm{Nd}}$. It will focus on how these methods will be used in this project and their limitations.

The volcanism section of the literature review begins with an outline of how ice sheets and volcanism interact during the recent past. It then looks at theories for how volcanism can be influenced by ice sheet volume, and how the iNHG could have influenced this. Finally, there is an examination of the methods that will be used, and the sites that we will be studying.

The final section of the report will outline how these knowledge gaps will be answered. It will look at the results that have been obtained already from oxygen isotope and trace metal analysis in the North Pacific and the questions raised by these results. This section will then point to the techniques and samples that will be analysed to infer how AMOC strength changed over the iNHG. Finally, there will be a discussion on the methods I will use to determine if rates of volcanism changed over the iNHG, as well what contingencies I will put in place if there is not sufficient tephra preserved at the site.

2 Literature Review

2.1 The Intensification of Northern Hemisphere Glaciation

The iNHG was a major shift in the Earth's climate and is marked by the growth of major ice sheets across Northern Eurasia and North America. It is not possible to exactly define the start, let alone the intensification, of ice sheet growth in the Northern Hemisphere. There is evidence for ephemeral ice sheets in Greenland from the Late Eocene (Eldrett et al., 2007), but there are no permanent ice sheets until the Late Pliocene, around 3.15 Ma (Bartoli et al., 2005). This Greenland ice sheet is a lot smaller, by a factor of about 50, than later Northern Hemisphere ice sheets (Batchelor et al., 2019), which do not appear for another 200 ka. The later ice sheet growth is commonly referred to as the iNHG. There is also evidence for growth of the Antarctic ice sheet over this period between 3.3 - 2.5 Ma (McKay et al., 2012).

The main evidence for the growth of ice sheets comes from ice-rafted detritus (IRD), large dropstones found in marine sediment cores, carried by icebergs into the deep ocean. Evidence from IRD implies that the presence of ice sheets around Northeast Asia at 2.75 Ma (Maslin et al., 1995), in Scandinavia and North East America around 2.72 Ma (Kleiven et al., 2002), and Alaska and North West America around 2.65 Ma (Maslin et al., 1996). Geochemical analysis of the provenance of IRD from North East American glaciation around 2.72 Ma has suggested that the IRD is actually the result of calving of the Greenland ice sheets and that IRD from North East America only appears around 2.64 Ma (Bailey et al., 2013). The provenance of IRD from other continents has not been analysed implying that these ages may not be wholly accurate.

The other evidence for major glaciation over the iNHG comes from the oxygen isotope record of seawater preserved in foraminifera. Heavier oxygen isotopes in seawater, indicative of greater global ice volume (see section 2.4.1), are recorded in two phases, from 2.92 - 2.82 Ma and 2.74 - 2.64 Ma (Bartoli et al., 2005). The evidence for ice growth from oxygen isotopes can constrain the timings of the glaciation, it does not indicate where the ice growing and therefore the oxygen isotopes and IRD evidence need to be used in tandem. The coupled IRD and oxygen isotope evidence suggests that the iNHG commenced in the Late Pliocene. Terrestrial ice sheets began to grow around 2.8 - 2.9 Ma reaching the oceans 100 ka later, around 2.75 Ma, in most of the Northern Hemisphere, but possibly only reaching the Eastern Seaboard of North America 100 ka later still (Raymo et al., 1992; Maslin et al., 1995).

The growth of ice sheets over the iNHG has a major impact on global sea levels as water was stored in ice sheets. Mean Pliocene sea levels have been estimated to have been 9 - 13.5 m higher than Pleistocene interglacial levels (Winnick and Caves, 2015). The uncertainty in these sea level estimates is quite large ($>$ 20 m) due to factors such as diagenesis of shell material and changes in seawater chemistry (Raymo et al., 2018), but overall point to higher sea levels prior to the iNHG.

The fall in sea levels was accompanied by a drop in average SST of 2 - 3°C (McClymont et al., 2020) over the iNHG. Global atmospheric CO_2 levels, recorded in boron isotopes in foraminifera, show a decrease from Late Pliocene values of 410 ppmv to 300 ppmv in the Early Pleistocene (Bartoli et al., 2011). Estimates from carbon isotopes in foraminifera (Pearson and Palmer, 2000) and alkenones (Badger et al., 2013) give lower CO_2 concentrations of 280 ppmv falling to 200 ppmv in the Early Pleistocene. Despite the difference in absolute values, these studies agree that there was a fall in atmospheric CO_2 concentrations over the iNHG by 25 - 30%. This decline in atmospheric CO_2 concentrations could be driven by an increase in sequestration of carbon in the deep oceans over the iNHG (Bartoli et al., 2011). A similar process is invoked to explain the decline in CO_2 levels on glacial-interglacial timescales in the Late Pleistocene (Sigman and Boyle, 2000; Sigman et al., 2010), however the mechanisms are unlikely to be the same as the structure of the Pliocene Ocean is considerably different to the modern.

2.2 Modern and Pliocene Ocean Circulation

2.2.1 Modern Ocean Circulation

The structure of the deep oceans can be traced due to the inability of seawater to easily mix with waters of different densities (Brown et al., 2001). Water masses with different densities are only able to mix if their temperatures or salinities converge or they are physically mixed by rough bathymetry (Furue and Endoh, 2005). This means that different water masses in the deep ocean can be tracked through their physical characteristics (figure 1).

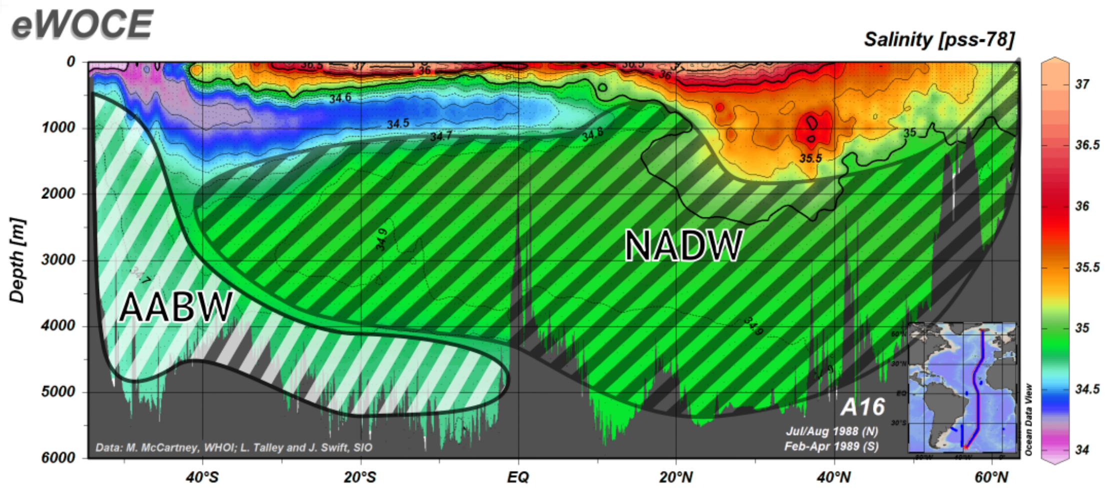

Figure 1: Salinity profile of the Atlantic Ocean from showing the distinct water masses identifiable by their salinity fingerprint. From Schlitzer (2000)

The structure of the deep oceans is defined by the formation of deep waters in the northern and southern high latitudes as surface waters cool, gain density, and sink to the deep ocean. This process occurs in the North Atlantic Ocean, forming North Atlantic Deep Water (NADW), and in the Southern Ocean, forming Antarctic Bottom Water (AABW) and Circumpolar Deep Water (CDW) (Talley et al., 2011). The very deepest parts of the South Atlantic are filled with AABW which is overlaid by NADW as it travels southwards (figure 1). The NADW is then upwelled in the Southern Ocean, where a component mixes with circumpolar waters to form CDW, and another component mixes with surface waters and is returned to the North Atlantic over the surface (Talley, 2013). The return of this water forms the Atlantic Meridional Overturning Circulation (AMOC) cell. The strength of the AMOC has been variable in recent geological history. The AMOC may have shutdown (Broecker et al., 1992) or significantly weakened (Oppo et al., 2015) during previous extreme glacial events, and may have strengthened relative to the present during the last interglacial (Guihou et al., 2011).

In the Southern Ocean, AABW is an incredible dense water mass that forms off the coast of Antarctica, and in gaps in the ice sheet called polynyas where fast cold winds can cool the surface waters very quickly. This results in very cold, very dense waters that entrain subsurface waters as they sink (Ohshima et al., 2016). CDW meanwhile forms in the surrounding Southern Ocean through mixing of upwelling waters with surface waters cooled by cold circumpolar wind currents, and is (relatively) warm and saline in comparison (Moffat et al., 2009). These two Southern Ocean water masses are then exported to the deep Atlantic, Pacific and Indian Oceans (figure 2).

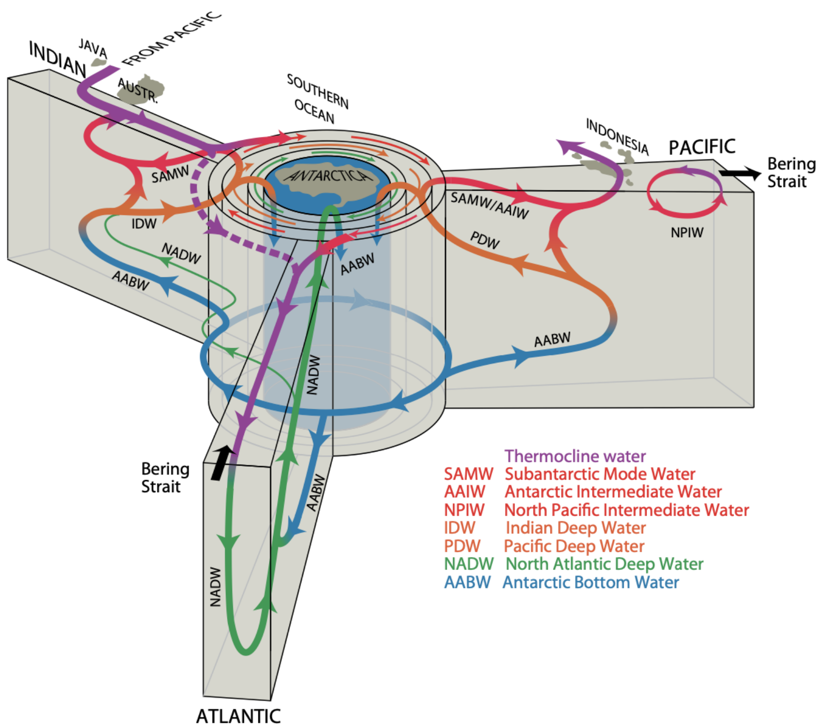

Figure 2: Schematic showing the paths of deep water masses around the world's oceans in the modern day. From Talley (2013)

Unlike the Southern and Atlantic Oceans, there are no deep waters that form in the Pacific Ocean. The surface waters of the subpolar North Pacific are as cold as the North Atlantic, but are relatively fresh and this keeps them too buoyant to sink to depth (Warren, 1983). The deep Pacific Ocean is therefore filled by waters sourced from the Southern Ocean. This mix of CDW and AABW fill the abyssal Pacific Ocean (figure 3), where they gradually warm and mix with fresher waters to lose density, rise, and form Pacific Deep Water (PDW) (Talley, 2013).

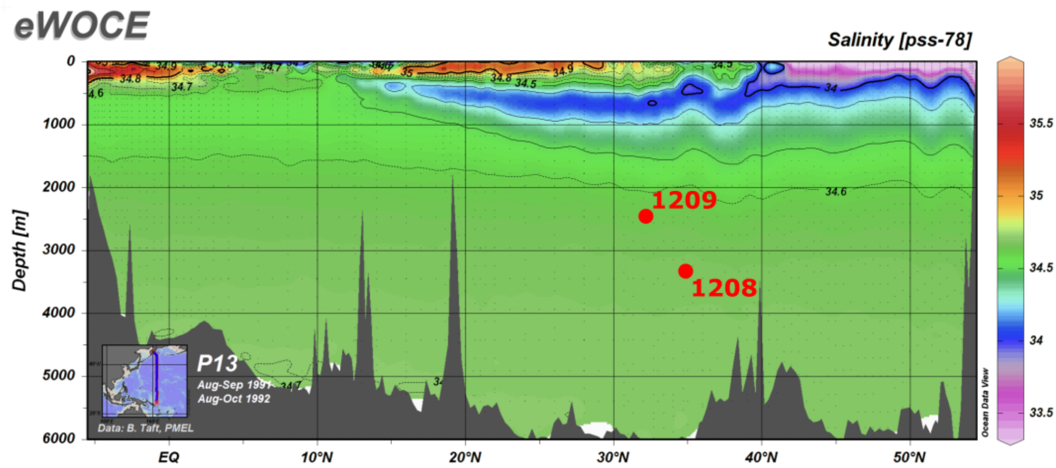

Figure 3: Salinity profile of the West Pacific Ocean showing the homogeneity in deep waters below 1000 m depth. Locations of ODP Sites 1208 and 1209 are marked in red. From Schlitzer (2000)

The strong salinity gradient in the North Pacific Ocean, or halocline, determines much of the structure of the deep Pacific Ocean. The cause of this halocline is not known, but suggestions include excess precipitation in the North Pacific (Stocker and Wright, 1991), exchange of waters from subpolar and subtropical ocean gyres (Emile-Geay, 2003), and the export of fresh waters from the Atlantic to the Pacific through atmospheric teleconnections over the Isthmus of Panama (Richter and Xie, 2010). The excess of precipitation over evaporation in the North Pacific has been attributed to moisture flux from the Asian Monsoon (Emile-Geay, 2003), the shape of the Pacific Ocean basin (Ferreira et al., 2018), or the strong SST gradient between the equatorial and subpolar Pacific Ocean (Burls et al., 2017).

While there is no deep water formation in the North Pacific, the cold but fresh waters of the subpolar North Pacific are able to sink to form North Pacific Intermediate Waters (NPIW), which do not extend below 1000 m depth (Talley, 1993). The formation of NPIW is unusual with cool subpolar waters being forced into the East Pacific before sinking to depth (You, 2003). NPIW is not dense enough to sink deeper than 1000 m and thus has little bearing on wider ocean circulation in the modern Pacific Ocean.

2.2.2 Pliocene Oceanography

In the Pliocene there are many indications that ocean circulation was fundamentally different, particularly in the Pacific Ocean. Pliocene SSTs were 2 - 3°C warmer than present and due to polar amplification, high latitude SSTs were around 10°C warmer than present (Wilson, 2011). This would markedly reduce the meridional (north-south) temperature gradient in the Pacific Ocean, which is been supported by SST proxies from the Pliocene (Fedorov et al., 2015). This reduced meridional SST gradient would decrease the amount of precipitation over the North Pacific and erode the strong halocline, which could allow for deep water formation in the Late Pliocene North Pacific (Burls et al., 2017) forming a Pacific Meridional Overturning Circulation (PMOC) cell (figure 4).

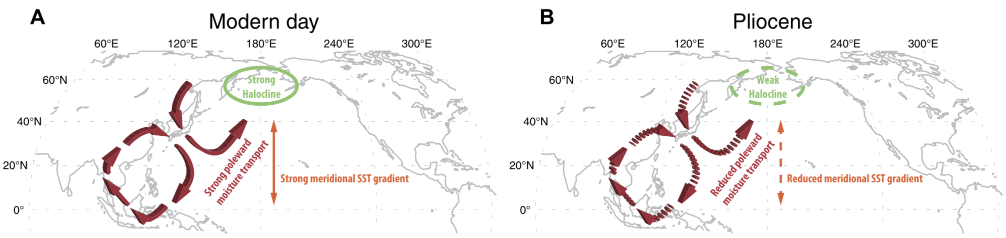

Figure 4: Schematic of the impact of a reduced Pacific SST gradient in the Late Pliocene on the North Pacific halocline allowing for PMOC formation. From Burls et al. (2017)

2.2.3 Pacific Meridional Overturning Circulation

The presence of a Pliocene PMOC is backed up by a range of paleo-proxy evidence. High diatom productivity, indicative of a strong nutrient flux and upwelling of deep waters, is seen in the North Pacific (Haug et al., 1999; Sigman et al., 2004). Upwelling waters in the North Pacific require surface waters to sink to depth to replace these, and suggest a reduced stratification in the subpolar North Pacific. This idea is supported by evidence from carbon isotopes which point to a more ventilated intermediate-depth North Pacific Ocean (Ford et al., 2022). The mechanism for formation of a PMOC suggests that a reduced meridional SST gradient causes reduced moisture transport to high latitudes which erodes the strong halocline in the North Pacific (Burls et al., 2017). The removal of this halocline would allow for the formation of North Pacific Deep Waters (NPDW) which would then upwell and form this PMOC cell (Menviel et al., 2012; Thomas et al., 2021). There is evidence for upwelling of nutrient-rich deep waters in the equatorial Pacific during the Pliocene (Shankle et al., 2021) thought to be this NPDW (Thomas et al., 2021). The NPDW that would form from an active PMOC would be a colder, but also slightly fresher, water mass compared to the CDW and AABW water masses in the deep Pacific Ocean (figure 5).

There is evidence that contradicts the idea of a Pliocene PMOC. Oxygen isotopes from sites in the North East Pacific Ocean show a fresher colder water mass overlying more saline waters, which could be explained by a PMOC, but also have carbon isotopes

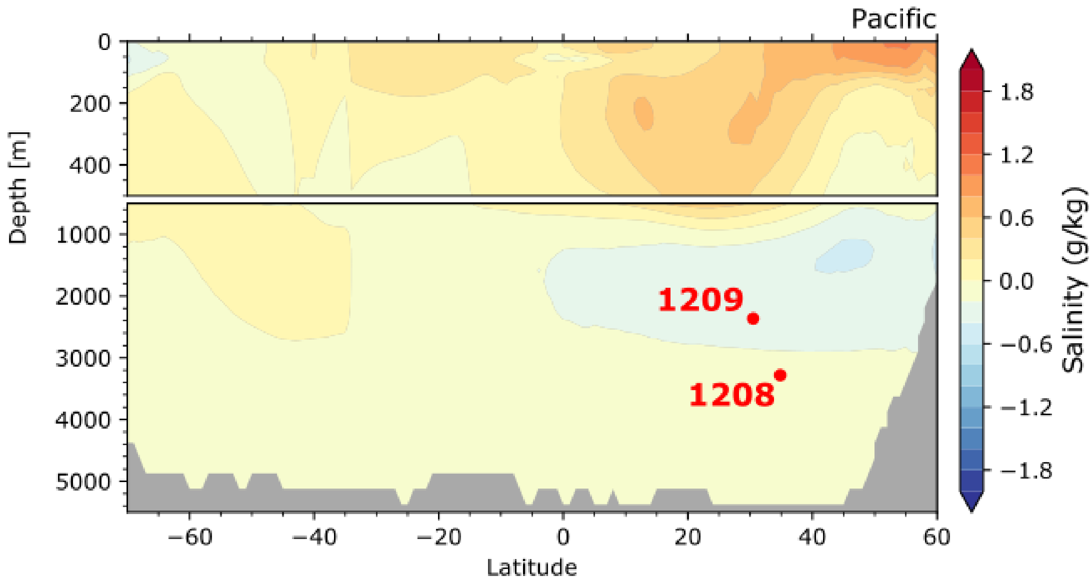

Figure 5: Model output showing salinity in the Pacific Ocean in the Late Pliocene relative to the preindustrial. Shown in red are the locations of ODP Sites 1208 and 1209. From Ford et al. (2022)

that suggest the shallower water mass was less ventilated than the deeper water mass, which does not fit with a PMOC (Kwiek and Ravelo, 1999). These results could be explained by the proximity of the sites to the California Margin which has occasional anoxic periods caused by high primary productivity, which would sway the carbon isotopes (Dean et al., 1997).

The evidence for the Pliocene PMOC is absent in the Pleistocene. North Pacific contourites, which can be used as a proxy for flow speed, suggest that deep ocean currents in the Pacific have got progressively stronger in stages since 5 Ma (Yin et al., 2022). If there was a PMOC shutdown over the iNHG, then this would decrease flow speeds in the deep Pacific Ocean, rather than have them continually increase. The contourites could be influenced by local flow factors rather than basin-wide circulation patterns or could be overprinted by erosion of the sediment which would generate inaccurate fast circulation signals (Stow et al., 2008).

Most climate models of the Late Pliocene, such as those in the PlioMIP2 model intercomparison project, are unable to generate a PMOC (Zhang et al., 2021; Haywood et al., 2020). It is possible to generate a PMOC in a climate model but this requires changing the forcings to remove the North Pacific halocline (Burls and Fedorov, 2014; Burls et al., 2017; Menviel et al., 2012). This indicates that there is no well-described mechanism for why a PMOC might form. Theoretical ocean models of the Pacific Ocean have event suggest that the shape of the Pacific Ocean, particularly the width of the Pacific basin relative to the Atlantic, would make it impossible for a PMOC to ever form (Jones and Cessi, 2017, 2016). The lack of a PMOC in climate models of the Late Pliocene does not explain the evidence for strong overturning in the North Pacific. Furthermore, there is evidence from the last glacial period of significant deep water formation in the North Pacific. Radiocarbon ventilation ages in the North Pacific show a marked drop down to 2700 m depth in the last deglaciation indicative of a sinking of NPIW to depths far beyond what is possible in the modern day (Okazaki et al., 2010). Neodymium and boron isotopes in the North Pacific corroborate this idea of an expanded intermediate or even deep water mass in the extending down to as far as 3400 m depth (Rae et al., 2014), and as far south as the Australian Coast (Struve et al., 2022). The suggestion of deep circulation in the Pacific for both past glacials and the Late Pliocene implies that there is no fundamental block to deep circulation, but this is instead a factor of a strong halocline in the modern North Pacific Ocean.

2.2.4 Atlantic Circulation

The warmer world of the Pliocene is thought to have had stronger overturning circulation and a greater export of NADW out of the North Atlantic (Raymo et al., 1996; Ravelo and Andreasen, 2000). There is strong evidence for a greater NADW in the Pliocene from carbon isotopes in the Southern Atlantic (Raymo et al., 1992) and neodymium isotopes in the mid-Atlantic (Frenz et al., 2006). Alkenone and planktic foraminiferal proxies show a reduced meridional SST gradient in the North Atlantic and a reduced nutrient content from an invigorated North Atlantic current, which is indicative of a stronger AMOC (Naafs et al., 2010; Karas et al., 2017). These results are supported by climate model outputs which point to a faster and more active overturning in the Atlantic during the warm Late Pliocene (Weiffenbach et al., 2022).

2.3 Influence of the iNHG on Ocean Circulation

2.3.1 Cessation of the PMOC

The evidence of a PMOC that comes from carbon isotopes and opal production is absent after the iNHG (Haug et al., 2005; Swann, 2010). This is accompanied by evidence from diatoms of a strong subpolar North Pacific halocline established at 2.73 Ma (Swann et al., 2006; Studer et al., 2012), which would suppress any deep water formation. The reason why this halocline forms is disputed.

A stronger halocline could be the result of global atmospheric cooling over the iNHG. This would increase the meridional SST gradient in the Pacific Ocean due to greater cooling at the poles than at the equator (Fedorov et al., 2015) and result in greater net precipitation in the North Pacific, strengthening the halocline (Brierley and Fedorov, 2010; Burls et al., 2017). The stronger halocline could also be the result of large ice sheets terminating in the Bering Sea and the Gulf of Alaska. These would bring a supply of freshwater to the North Pacific which could strengthen the halocline, as has been suggested for the last glacial period (Praetorius et al., 2020). However, the first IRD evidence for marine-terminating ice sheets in Alaska is only found after 2.65 Ma

(Maslin et al., 1996), approximately 100 ka after the establishment of a permanent North Pacific halocline.

The establishment of a halocline may also have been driven by tectonic forcings. The final closure of the Central American Seaway (CAS) separating North and South America occurred by 2.7 Ma. This can be seen in fossil evidence for the exchange of vertebrate species between the two continents (Molnar, 2008). The coincident timing of the closure of the CAS and the cessation of the PMOC could imply a link. Climate models have suggested that with the closure of the seaway, warm and saline waters from the Caribbean Sea and the Gulf of Mexico would be transported to the North Atlantic rather than the North Pacific, freshening the surface North Pacific (Brierley and Fedorov, 2016). However, while the final closure of the CAS occurred at 2.7 Ma, the seaway was likely closed to deep water transport much earlier. Evidence from neodymium isotopes suggest the seaway may have closed as early as 10 Ma (Sepulchre et al., 2014), though most other evidence suggests that significant water mass transport through the CAS was stopped by 5-3 Ma (Molnar, 2008). These timings suggest that the closure of the CAS is unlikely to play a role in the cessation of the PMOC over the iNHG.

Modelling evidence has also pointed to the importance of the Bering Strait in modulating salinity in the North Pacific (Hu et al., 2012a; Otto-Bliesner et al., 2017). The Bering Strait currently allows for the export of fresh waters out of the Pacific Ocean into the North Atlantic (Hu and Meehl, 2005). Closure of these straits would result in a freshening of the North Pacific and strengthen the subpolar North Pacific halocline. There is evidence for the first shallow opening of the Bering Strait from 5.3 Ma (Gladenkov et al., 2002), but it would be closer to 4.8 Ma before there was significant exchange of water through the strait (Marincovich and Gladenkov, 1999). The shallowness of the Bering Strait means that only 0.8 Sv is transport through the strait in the present day (Hu et al., 2012b), but climate models have shown that this can have a major effect on deep ocean circulation (Brierley and Fedorov, 2016; Otto-Bliesner et al., 2017). The shallowness of the Bering Strait means that this process is also highly dependent on sea level (Hu et al., 2010). The sea level fluctuations over the iNHG could therefore have played a key role in suppressing the PMOC.

It seems likely that the PMOC is shutdown over the iNHG due to the establishment of a strong halocline in the North Pacific. However, the response of the deep Pacific Ocean to this halocline is poorly understood. Understanding the causes of, and responses to, the decline of the PMOC would also aid in our understanding of the mechanisms that were driving it.

2.3.2 Wider Oceanographic Changes

Outside the changes to the PMOC, the iNHG sees some wider oceanographic changes in the Pacific and Atlantic Oceans. There is evidence from Mg/Ca ratios in benthic foraminifera which show a convergence in bottom-water temperatures (BWT) between the deep Atlantic and Pacific Oceans over the iNHG (Woodard et al., 2014). This convergence in water mass properties between the deep Pacific and Atlantic Oceans might be the result of ice sheet and sea ice growth on Antarctica (Woodard et al., 2014).

The expanded Antarctic ice sheet would result in more CDW formation and export to both the Atlantic and Pacific Oceans, resulting in a more homogenous, "Antarctic", BWT signal in both oceans (Hill et al., 2017). Carbon and oxygen isotopes from the Plio-Pleistocene point to the presence of two distinct southern-sourced water masses in the South Atlantic over the iNHG, which may represent CDW water masses sourced from different parts of Antarctica (van der Weijst et al., 2020). The convergence of the BWT signals in the North Pacific and Atlantic Oceans could be the result of a PMOC shutdown, and a weaker AMOC, which would result in a more "Southern Ocean" signal in both oceans without the need for stronger CDW export. The accuracy of the North Atlantic BWT estimates has also been questioned due to the influenced of local carbonate ion saturation (Yu and Broecker, 2010; Sosdian and Rosenthal, 2010, 2009).

Alternatively, a stronger AMOC in the North Atlantic over the iNHG could result in more NADW-like BWT signal being exported to the Pacific Ocean after the iNHG (Kwiek and Ravelo, 1999). Proxy studies from the North Atlantic indicate that AMOC strength may have increased over the iNHG (Hayashi et al., 2020). However, there is evidence from carbon and neodymium isotopes in the mid and South Atlantic that AMOC strength is weakened over the iNHG (Hodell and Venz, 1992; Lang et al., 2016), which would undermine this theory.

2.4 Oceanographic Techniques

Understanding how ocean circulation has changed requires the ability to trace past water masses. This can be done through a variety of proxies for water mass characteristics. Carbon and oxygen isotopes in foraminifera can tell us about the productivity, salinity, and temperature of past water masses. The trace metal ratios of foraminiferal tests are able to indicate how the temperature and carbon state of water masses changed over time. These proxies tell us about water mass properties that are generally well conserved by water masses as they travel through the oceans. This allows them to be used as identifiers of distinct water masses (Kim et al., 2005; Rae et al., 2014; Woodard et al., 2014). Neodymium isotopes can be used to show the provenance of different water masses (Amakawa et al., 2004). The original signals in all of these proxies are prone overprinting by local signals and thus are often used in conjunction with each other to get a clearer picture of past ocean circulation.

2.4.1 Oxygen Isotopes and Salinity

Oxygen (and carbon) isotopes have been one of the most important techniques in oceanography dating back to the 1950s. The ratio of the stable isotopes of oxygen, ^{18}O and ^{16}O, in the carbonate tests of foraminifera can be used to infer the temperature of formation of the test as well as giving an indication of the global ice volume (Criss, 1999). This is often denoted by $\delta^{18}O$ which is defined as:

$$\delta^{18}\mathrm{O} = \left(\frac{\left(\frac{^{18}\mathrm{O}}{^{16}\mathrm{O}}\right)_{\mathrm{sample}}}{\left(\frac{^{18}O}{^{16}\mathrm{O}}\right)_{\mathrm{standard}}} - 1 \right) \times 1000 \tag{1}$$

The lighter isotopes of oxygen are preferentially fractionated into water vapour, and not into precipitation, resulting in lighter isotopes preferentially travelling to higher latitudes (Ravelo and Hillaire-Marcel, 2007). As these lighter isotopes are then preferentially trapped in ice sheets, this allows the resultant oxygen isotope ratio of sea water to reflect the global ice volume (Shackleton, 1987). The formation of calcite from seawater by foraminifera further fractionates these oxygen isotopes, with the degree of fractionation controlled by the temperature of the surrounding seawater (Ravelo and Hillaire-Marcel, 2007). Therefore, δ^{18}O measurements from foraminifera can broadly be used as a proxy for local temperature and global ice volume.

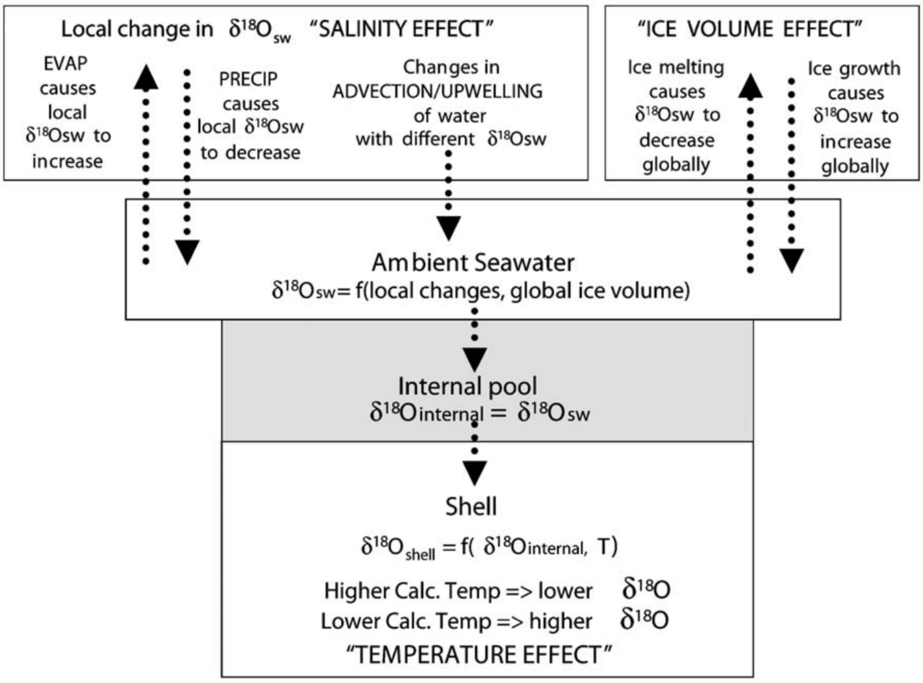

Figure 6: Environmental factors that influence the δ^{18}O of calcite in benthic foraminifera. From Ravelo and Hillaire-Marcel (2007)

There are many more smaller effects that can affect the resultant δ^{18}O of foraminiferal calcite (figure 6). The most important of these is the "salinity effect", where local precipitation causes changes to both the salinity and δ^{18}O values of the seawater (Benway and Mix, 2004). The surface salinity is then conserved as these surface waters sink to form deep waters, allowing oxygen isotopes to act as a proxy for salinity, and a water mass tracer.

As $\delta^{18}O$ measures both local temperature and salinity of water masses, it can be thought of as a proxy for density (Gu et al., 2019). Higher $\delta^{18}O$ values correspond to colder or more saline water masses, and therefore also more dense waters. However, it is possible to decouple $\delta^{18}O$ values from density through processes such as sea ice formation, which reject brine from formation but do not fractionate oxygen isotopes (Gebbie and Huybers, 2006). In the South Atlantic there is evidence of waters with higher $\delta^{18}O$ values sourced from the North Atlantic overlying lower $\delta^{18}O$ Southern Ocean waters (Lynch-Stieglitz et al., 2006) which is thought to represent the impact of sea ice formation on generation of very cold deep waters off the coast of Antarctica (Toggweiler and Samuels, 1995). While the correlation between $\delta^{18}O$ values and salinity is generally only applicable at very small scales (Conroy et al., 2014), the use of oxygen isotopes as a salinity proxy can still be useful - particularly if coupled with an independent measure of bottom-water temperatures.

2.4.2 Magnesium Calcium Ratios and Bottom Water Temperatures

The ratio of Mg^{2+} to Ca^{2+} ions in calcite has been used as a proxy for past ocean temperatures in the tests of corals (Ross et al., 2019), ostracods (Rodríguez-Tovar et al., 2019), and planktic (Holland et al., 2020) and benthic (Barrientos et al., 2018) foraminifera. The advantage of this method compared to other palaeothermometers such as alkenones is the ability to measure ambient temperatures around benthic foraminifera, and thus determine bottom water temperatures.

The principle of Mg/Ca ratios in foraminifera is that foraminiferal tests are built of calcite, $CaCO_3$, but the Ca^{2+} ion can be substituted for Mg^{2+} ion to form $MgCO_3$. This substitution is an endothermic reaction and thus is favoured at higher temperatures (Elstnerová et al., 2010). In a completely inorganic system, it is possible to determine the degree of Mg substitution using the enthalpies of formation of $MgCO_3$ and $CaCO_3$, which should increase exponentially with temperature (Rosenthal et al., 1997). However, in biogenic calcite, there are significant vital controls on this process, resulting in much lower but also much more temperature dependent Mg^{2+} incorporation into calcite (Martin et al., 2002; Bentov and Erez, 2006). This biogenic control on the incorporation of Mg^{2+} ions could be achieved through amorphous secondary phases from which calcite tests grow, involvement of an organic matrix to filter out unwanted ions, or pumping ions out of the parent solution to reduce local Mg^{2+} concentrations (Bentov and Erez, 2006; Erez, 2003). Nano-scale x-ray spectroscopy points to continuous incorporation of Mg^{2+} into foraminiferal calcite suggesting that it is likely that the calcite grows in one phase and therefore that we can still use linear or exponential relationships between temperature and Mg/Ca despite these vital effects (Branson et al., 2013). However, these vital effects can differ between species, and occasionally between morphotypes, of foraminifera (Steinke et al., 2005; Schmitt et al., 2019).

To determine a temperature of shell formation from the Mg/Ca ratio requires species specific calibrations between formation temperature and Mg/Ca ratios. While planktic foraminifera can be grown in a laboratory setting (Gray and Evans, 2019) to study the non-thermal influences on Mg/Ca and determine the temperature calibration, for benthic species the only way to do this is through core-top studies (Lea, 2014). Core-top studies from benthic foraminifera are able to come up with region specific as well as species specific calibrations, such as this calibration for Uvigerina peregrina in the tropical Pacific Ocean (Stirpe et al., 2021). The relationship between Mg/Ca and temperature varies between exponential and linear relationships for different species and temperature ranges (figure 7) (Elderfield et al., 2006).

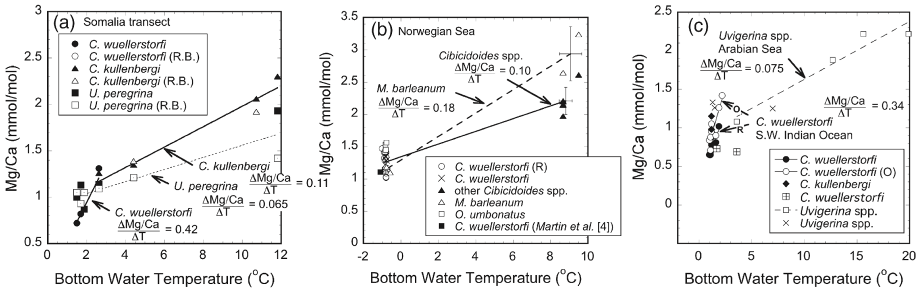

Figure 7: Mg/Ca-BWT calibrations for benthic foraminifera species from different ocean basins. From Elderfield et al. (2006)

There are a variety of non-thermal controls on Mg/Ca incorporation into calcite. There are suggestions that Mg/Ca ratios can decrease with increasing water depth (Lea, 2014) and salinity (Dissard et al., 2010). The problem with Mg/Ca is that Mg^{2+} concentrations are often very low, with concentrations of less than 0.3% by weight (Emiliani, 1955), and therefore dissolution of part of a calcite shell can have marked changes on resultant Mg/Ca ratios (Barker et al., 2003). There are suggestions that Mg^{2+} enriched sections of calcite tests are more prone to dissolution compared to normal calcite, which would preferentially lower Mg/Ca ratios with increased dissolution (Brown and Elderfield, 1996).

Carbonate ion concentration, $\Delta\left[CO_3^-\right]$, also has a control on Mg/Ca ratios in certain benthic foraminifera (Rosenthal et al., 2006). Most notably, the Mg/Ca ratios from *Cibicidoides wuellerstorfi*, a species often used for oxygen and carbon isotope studies, has been shown to be independent of temperature, and solely dependent on $\Delta\left[CO_3^-\right]$ (Yu and Elderfield, 2008). Selection of specific benthic foraminifera species, such as *Uvigerina* (Elderfield et al., 2006), or *Oridorsalis umbonatus* (Lear et al., 2015), which are not affected by $\Delta\left[CO_3^-\right]$ is therefore required to obtain reliable BWT estimates.

A final control on Mg/Ca ratios is the Mg/Ca ratio of the seawater (Mg/Ca_{sw}), which can bias temperature reconstructions (Lea, 2014). The residence time of Mg^{2+} in the oceans, ∼10 Myr (Hem, 1985), is much longer than the age of the iNHG, and thus the Mg/Ca_{sw} is unlikely to have changed markedly since the Pliocene. Evidence to suggest that the Mg/Ca_{sw} was around 5.2 mol mol^{-1} during the mPWP, compared to the present value of 3 - 4 mol mol^{-1} (Evans et al., 2016). Assuming Mg/Ca_{sw} has linearly decreased from the Pliocene to the present, it is possible to correct Pliocene Mg/Ca ratios for this Mg/Ca$_{sw}$ offset (Evans et al., 2016; Jakob et al., 2020).

Even with the correct species of foraminifera and corrections for non-thermal factors, Mg/Ca measurements are prone to error from contamination. Accurate Mg/Ca measurements therefore rely thorough oxidative and reductive cleaning of foraminifera samples prior to measurement (Boyle and Keigwin, 1985; Barker et al., 2003). The reductive cleaning steps can result in dissolution of sample and lower Mg/Ca ratios (Elderfield et al., 2006; Yu et al., 2007), but are shown to remove most contaminants that could influence the final result (Weldeab et al., 2006).

The strength of Mg/Ca as a proxy is beyond just accurate BWT estimates. As deep-water temperatures only change when they are exposed to the surface or through mixing with other water masses, Mg/Ca derived BWT can be used as a semi-conservative water mass tracer (Woodard et al., 2014; Jakob et al., 2021). As explained earlier, the δ^{18}O composition of benthic foraminiferal tests ($\delta^{18}O_{benthic}$) is a measure of both local BWT and the δ^{18}O of seawater ($\delta^{18}O_{sw}$). Mg/Ca is an independent measure of BWT, allowing coupled Mg/Ca-δ^{18}O measurements to resolve the temperature dependence of $\delta^{18}O_{benthic}$ to give the $\delta^{18}O_{sw}$ at the time of formation of the test, and therefore more accurate estimates of global ice volume (Elderfield et al., 2012; Raymo et al., 2018). The difference between the global average $\delta^{18}O_{sw}$ and local $\delta^{18}O_{sw}$ is a function of regional hydrological changes (Gonfiantini et al., 2020), allowing coupled Mg/Ca-$\delta^{18}O_{benthic}$ measurements to be used as a paleo-salinity proxy in planktic foraminifera (Flower et al., 2004; Schmidt et al., 2004; Nürnberg et al., 2008).

2.4.3 Boron Calcium Ratios and Carbonate Ion Concentrations

The ratio of boron to calcium in calcite can be used as a proxy for the carbonate ion saturation of seawater (Hönisch et al., 2019). This is based on the idea that boron, or more specifically borate, $B(OH)_4^-$, can be incorporated into calcite in place of carbonate:

$$CaCO_{3_{solid}} + B(OH)^-_{4_{aq}} \leftrightarrow CaHBO_{3_{solid}} + HCO^-_{3_{aq}} + H_2O_{aq} \tag{2}$$

The B/Ca ratio should then be a function of the concentration of boron, $[B_T]$, and bicarbonate, $[HCO_3]$, in seawater (Yu and Elderfield, 2007). Empirical studies of core-top conditions and B/Ca ratios show a strong relationship between B/Ca in calcite and $\Delta\left[CO_3^-\right]$ (Yu and Elderfield, 2007; Rae et al., 2011). The relationship between B/Ca and $\Delta\left[CO_3^-\right]$ is dependent on species, and sometimes even morphotypes within species (figure 8), suggesting a strong physiological control on boron incorporation into foraminiferal calcite (Rae et al., 2011).

The $\Delta\left[CO_3^-\right]$ describes the difference between the bottom water carbonate concentration and the saturation concentration at that location:

$$\Delta\left[CO_3^-\right] = \left[CO_3^-\right]_{\text{in situ}} - \left[CO_3^-\right]_{\text{saturation}} \tag{3}$$

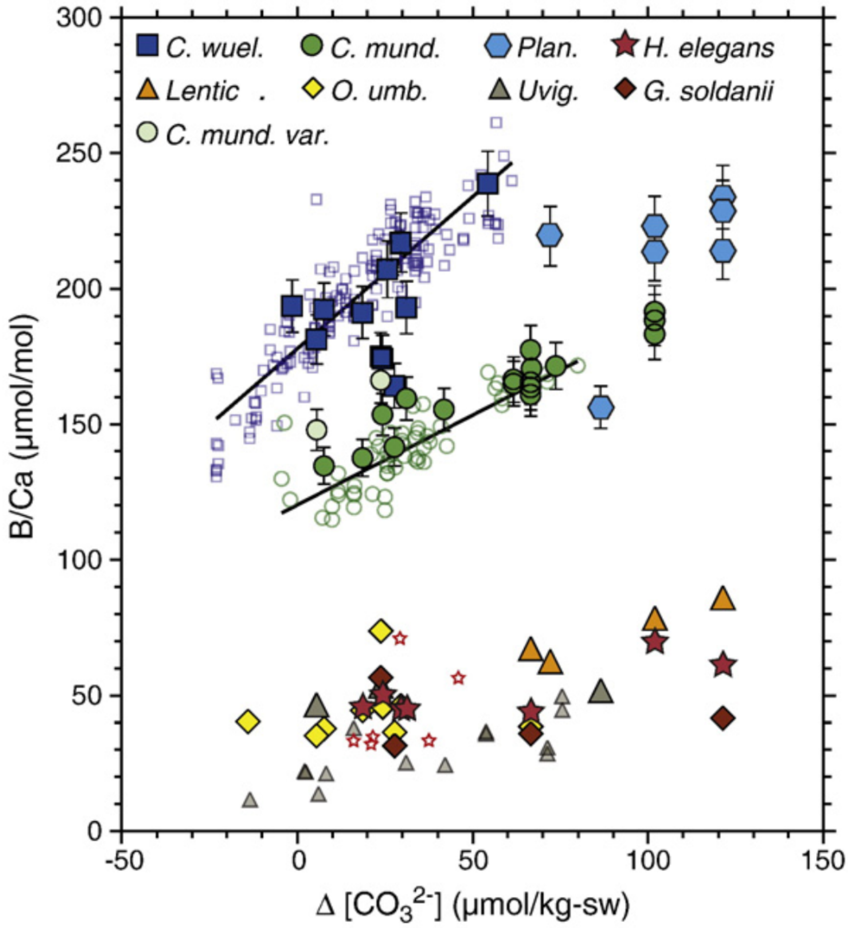

Figure 8: Relationship between B/Ca and $\Delta\left[CO_3^-\right]$ for various benthic foraminifera species and morphotypes of *C. mundulus*. From Rae et al. (2011)

The $\left[CO_3^-\right]_{saturation}$ is a function of the depth, pressure, and salinity (Lynch-Stieglitz, 2004). Knowledge of these water mass properties allows us to estimate the $\left[CO_3^-\right]$ of seawater (Yu and Elderfield, 2007). While the depth of a particular site is often known for at least the last 10 million years, the salinity, and thus $\left[CO_3^-\right]_{saturation}$, of past water masses can only be reliably estimated for a few hundred thousand years (Hönisch et al., 2019). For further into deep time, B/Ca carbonate reconstructions require estimates of past salinity, which could be derived from coupled Mg/Ca-δ^{18}O measurements (see section: 2.4.2) and estimates of seawater boron concentration (Tripati et al., 2009).

Using B/Ca ratios to estimate past carbonate concentration can be influenced by the boron concentration in seawater (Uchikawa et al., 2017, 2015). The residence time of boron in the oceans is between 10 and 20 Myr (Crumpton-Banks and Rae, 2020). This means that total boron concentration in seawater is not believed to have changed considerably on Pliocene timescales, and the total boron concentration can be effectively modelled for this timescale (Lemarchand et al., 2000, 2002).

The ocean carbonate system can be defined by 4 independent equations with 6 components (Irving, 1925), shown below:

$$CO_2 + H_2O \leftrightarrow H_2CO_3 \tag{4}$$

$$H_2CO_3 \leftrightarrow HCO_3^- + H^+ \tag{5}$$

$$HCO_3^- + H^+ \leftrightarrow CO_3^{2-} + 2H^+ \tag{6}$$

$$H_2O \leftrightarrow H^+ + OH^- \tag{7}$$

Therefore, if two of these components are known it is possible to infer the state of the carbonate system at this location. B/Ca provide knowledge of one of these components, $\left[CO_3^-\right]$, but requires another measurement to determine the whole system. This could be $\delta^{11}B$ measurements to infer past pH (Foster, 2008), or modelling past carbonate ion ratios (Tripati et al., 2009) to solve this issue.

Knowledge of the carbonate concentration of deep-waters can be used to infer carbon storage in the abyssal oceans allowing for estimates of past atmospheric CO_2 concentrations (Tripati et al., 2009; Chalk et al., 2019). B/Ca ratios can also be used to estimate the circulation of carbon through an ocean reservoir (Yu et al., 2008, 2014). As carbonate concentration in deep-waters only changes with surface exchange or through mixing with other water masses, it is also possible to use B/Ca as a semi-conservative water mass tracer akin to $\delta^{13}C$ measurements (Chalk et al., 2019).

2.4.4 Neodymium Isotopes as a water mass tracer

Seeing how the strength of deep water formation has changed over time can be most easily achieved through examining the spatial extent of water masses. All else being equal, a stronger AMOC would result in a greater NADW extent, while a weaker PMOC would result in a reduced NPDW extent. The relative proportions of isotopes of neodymium (Nd) within the authigenic fraction of ocean sediments provides an archive of past seawater compositions which can be translated into an estimate of water mass extent.

Since Nd isotopes, and specifically ^{143}Nd and ^{144}Nd, do not fractionate within sediments (Bizimis and Scher, 2016), the difference in isotope concentrations is primarily due to the decay of ^{147}Sm into ^{143}Nd (Lugmair and Scheinin, 1974). Samarium is slightly less incompatible than neodymium during mantle melting, so the Sm/Nd ratio in mantle melts is lower than in the mantle residue. This residue forms continental rocks which then have a lower Sm/Nd ratio, and over time this will result in a lower $^{143}Nd/^{144}Nd$ ratio compared to igneous rocks (Bizimis and Scher, 2016). The ratio of neodymium isotopes is often expressed as ε_{Nd}, the ratio of $^{143}Nd/^{144}Nd$ relative to the bulk silicate Earth (Goldstein and Hemming, 2003) as below:

$$\varepsilon_{Nd} = \left[\left\{\frac{(^{143}Nd/^{144}Nd)_{sample}}{(^{143}Nd/^{144}Nd)_{bulk\ Earth}}\right\} - 1\right] \times 10^4 \tag{8}$$

Older cratonic rocks will have negative $\varepsilon_{\mathrm{Nd}}$ values, while younger volcanic rocks will have positive values (Lambelet et al., 2016). As these rocks are weathered, the physical products end up as sediments in the ocean. The Nd that is released in dissolved form retains the $\varepsilon_{\mathrm{Nd}}$ value of the original sediments and imparts this signature to the ocean. Therefore, water masses surrounded by younger rocks, such as the Pacific Ocean, usually have more positive $\varepsilon_{\mathrm{Nd}}$ values compared to those found in the North Atlantic Ocean (Goldstein and Hemming, 2003). This is supported by modern observations of seawater composition (figure 9).

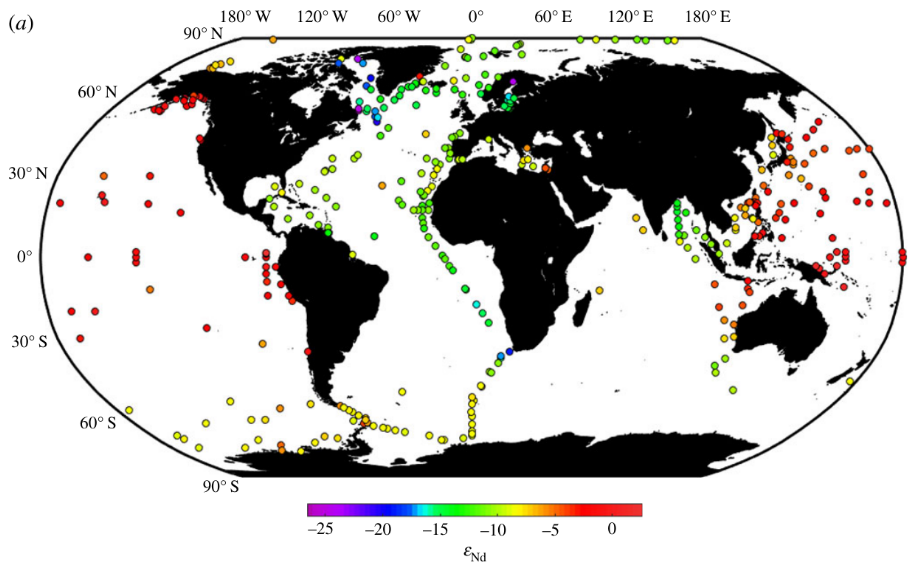

Figure 9: Map of modern seawater $\varepsilon_{\mathrm{Nd}}$ values from ocean cruises, many of which were conducted as part of the GEOTRACES project (van de Flierdt et al., 2016)

Deep water formation only occurs in a few specific places (Gebbie and Huybers, 2011). The surface water $\varepsilon_{\mathrm{Nd}}$ value at these deep water formation sites determines the eventual deep waters that form. The residence time of Nd in the oceans is about 200 - 1000 years (Tachikawa et al., 1999), and shorter than the overturning time of the oceans. This means that Nd is not well mixed in the oceans, but varies spatially, which can be used to trace water mass origins (Bizimis and Scher, 2016).

The Nd isotope composition of deep waters can be recorded in authigenic sediments that precipitate out of seawater. Commonly used archives include fish teeth (Osborne et al., 2014), corals (van de Flierdt et al., 2006), and foraminifera (Tachikawa et al., 2014). Coupled with accurate age models, these Nd records can show how relative proportions of water masses have changed over time at certain locations.

Determining the provenance of past water masses from $\varepsilon_{\mathrm{Nd}}$ measurements requires a knowledge of past end member $\varepsilon_{\mathrm{Nd}}$ compositions, the $\varepsilon_{\mathrm{Nd}}$ values for the surface waters. This is well constrained for the modern day (van de Flierdt et al., 2016), but may have changed in the past in ways that are difficult to model (figure 10).

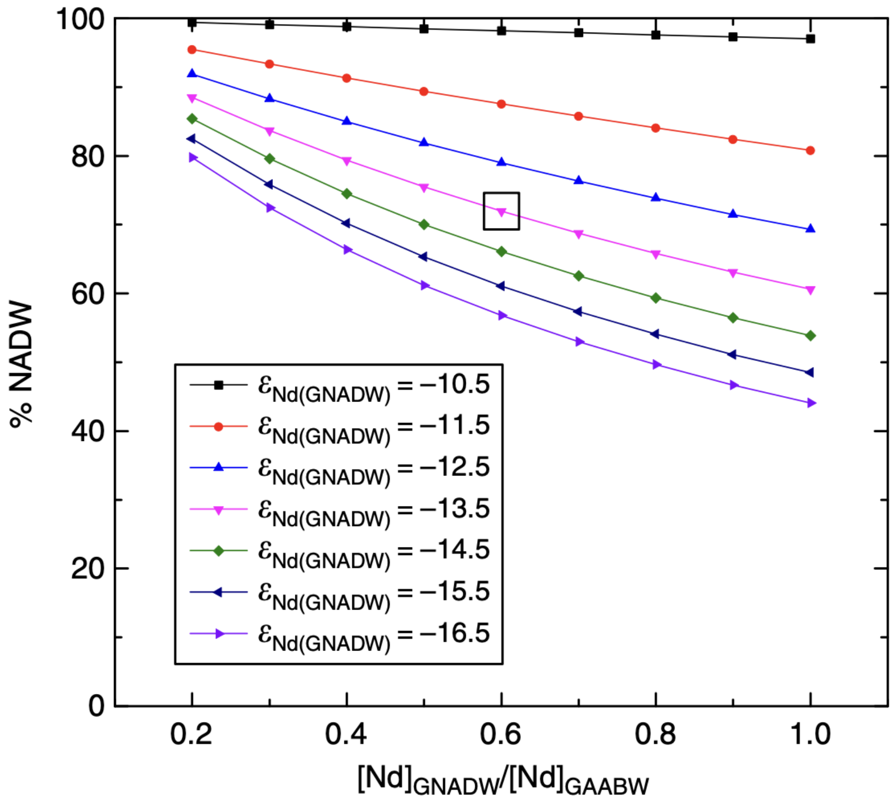

Figure 10: Estimates of the percentage of NADW at a site in the deep North Atlantic during the Last Glacial Maximum for a range of different end-member NADW ε_{Nd} compositions and Nd concentrations (Howe et al., 2016)

Determining past circulation patterns based on estimates of endmember ε_{Nd} values is further complicated by the fact that deep water masses have not always have formed in the same places as today. How relative contributions of ISOW, DSOW, and LSW to deep waters forming in the North Atlantic has changed in the past is still poorly constrained for the last glacial limiting the effectiveness of ε_{Nd} as a tracer of water mass extent (Dokken and Jansen, 1999; Hillaire-Marcel et al., 2001; Crocket et al., 2011; Larkin et al., 2022). When coupled with other semi-conservative water mass tracers, such as oxygen isotopes, Mg/Ca, and B/Ca measurements, ε_{Nd} measurements can be used to deconvolve the relative contributions of these components of deep water masses.

Even if we could perfectly model the formation of past deep water masses, reconstructing circulation through ε_{Nd} measurements still faces several hurdles. Simple interpretations of water mass mixing based on ε_{Nd} rely on Nd behaving as a conservative element within the oceans, despite the evidence to suggest otherwise (Lacan and Jeandel, 2005; Jeandel, 2016; Jeandel et al., 2007; Haley et al., 2017). This is primarily due to boundary exchange and benthic flux.

Particles are able to scavenge Nd from the water column, which removes the total Nd concentration in the oceans in a process referred to as boundary exchange (Jeandel, 2016). This does not directly affect the $\varepsilon_{\mathrm{Nd}}$ value but makes seawater $\varepsilon_{\mathrm{Nd}}$ values more prone to isotopic shifts caused by the transport of continental-derived sediments to the deep ocean which can then dissolve and change deep ocean $\varepsilon_{\mathrm{Nd}}$. This is benthic flux (Du et al., 2016; Abbott et al., 2015). Together these two processes can markedly change seawater $\varepsilon_{\mathrm{Nd}}$ values. The effects of benthic flux and boundary exchange can be limited through empirical modelling of sedimentary fluxes within the ocean (Haley et al., 2017; Pöppelmeier et al., 2022).

Neodymium isotopes can be used to determine the extent of water masses in the ocean, which can be used to infer the strength of overturning circulation cells, such as the AMOC or PMOC. The extent of water masses such as NADW is not only a factor of AMOC strength but also export of Southern Ocean deep water masses which limits how much can be inferred from these isotopes in isolation (Lang et al., 2016). In combination with flow speed proxies, such as sortable silt, or Pa/Th, it may be possible to infer past overturning strength (Jonkers et al., 2015).

2.5 The Impact of the iNHG on Volcanism

2.5.1 The Interaction between Volcanism and the Climate

Volcanic eruptions are the result of tectonic plate movements on geological timescales. Plate movements allow cracks to develop in the Earth's lithosphere, through which magma can rise. As it does so, the lower pressure melts the magma resulting in volcanism. This volcanism can play a major role in shaping the Earth's climate by releasing greenhouse gases and aerosols into the atmosphere (Hay, 1996; Kender et al., 2021). This can occur on the annual timescales for sulphate aerosols (Zhu et al., 2020), or multi-millennial timescales or longer for CO_2 emissions and changes to the carbon cycle (Sigl et al., 2015; Lohmann and Svensson, 2022). The influence of volcanism on the climate highlights the importance of understanding the triggers for volcanism.

Volcanism can have an impact on the climate, but it is also possible for climate shifts to influence rates of volcanism. This is predominately done through the movement of ice sheets which place large stresses on the lithosphere (Nakada and Yokose, 1992). Rates of volcanism on Iceland were found to be considerably higher during the end of the last glacial than during the period before or after (Maclennan et al., 2002). This is linked to the removal of the ice sheet over Iceland following the deglaciation resulting in a reduction of pressure on the crust, increasing the rate of magma melting and thus volcanism (Aubry et al., 2022). This relationship is less straightforward with arc volcanism potentially due to deeper magma chambers (Watt et al., 2013). There is also a suggestion that sea level changes can influence volcanism through increased stress on mid-ocean ridges (Boulahanis et al., 2020). On longer timescales, it is possible to observe pulses in the rates of volcanism which correspond to orbital timescales, suggesting that volcanism may be influenced by ice sheets outside the last deglacial (Schindlbeck et al., 2018).

2.5.2 The Influence of the iNHG on Volcanism

The iNHG represents an increase in ice volume across much of the Northern Hemisphere. The increased loading from ice sheets could result in a reduction in the eruption rate due to greater stress on the lithosphere increasing the pressure on the magma chamber and thus reducing melting. Alternatively, compared to the lack of Pliocene ice sheets in the Northern Hemisphere (Hill et al., 2007), the rapidly retreating and advancing ice sheets of the Pleistocene could induce volcanism through fracturing of the crust and allowing more paths for magma to ascend and then melt. Therefore, it would be the rate of change of ice volume rather than the removal of ice volume that could influence the eruption rate (Jellinek et al., 2004). It has been suggested that the increased volcanism in Eastern California during Pleistocene interglacials may have been triggered by ice advance (Glazner et al., 1999). This increased fracturing of the crust could also lead to more dyke emplacement allowing for release of pressure from the magma chamber prior to eruption, reducing the rate of eruptions (Sigmundsson et al., 2010). At the scale of single volcanoes, the shape of individual magma chambers can introduce significant heterogeneities in the rates of magmatism (Sigmundsson et al., 2012).

Evidence does suggest that there is increased volcanism in the Pleistocene compared to previous epochs which could be the result of increased ice sheet loading (Kennett and Thunell, 1975). However, this may also be an artefact of greater preservation of more recent sediments (Hawkesworth et al., 2009).

Previous studies have yet to look at the impact of the iNHG on volcanism. There is an increase in tephra layers recorded in North Pacific sediments around 2.65 Ma (Prueher and Rea, 1998, 2001), which occurs before the appearance of IRD, evidence of widespread glaciation. This suggests that locally to the North Pacific, volcanism may have been a cause, rather than an effect, of the increased glaciation (Prueher and Rea, 1998). There is evidence from the North Atlantic suggesting an increase in tephra layers in the Late Pliocene, potentially linked to the growing ice sheets (Lacasse and van den Bogaard, 2002). There is no synchronous increase in terrestrial deposition of tephra on Iceland over the Late Pliocene (Geirsdóttir and Eiríksson, 1994) indicating that this increase may not be the result of an increased rate of volcanism.

2.5.3 Changes in the Rate of Volcanism

Determining past changes in rates of volcanism measured in the accumulation of tephra. Tephra describes siliciclastic ejecta from volcanic eruptions, layers of which can be buried in the sediment and become part of the stratigraphy. Greater numbers of tephra layers can be used as an indicator of increased volcanism (Kutterolf et al., 2019). Geochemical analysis of tephra layers allows layers to be tied to specific volcanic eruptions (Bourne et al., 2015), or magmatic processes (Maclennan et al., 2002), allowing for inferences on the causes of change of rates of volcanism.

Tephra analysis in marine sedimentary sequences, either visually or geochemically, requires the extraction of vitreous glass shards from the sediment (Blockley et al., 2005). Tephra is made of predominately volcanic glasses, which are prone to dissolution, removing all visible traces of the original tephra layer. Observations of cryptotephra layers, layers which contain so few glass shards that they are invisible to the naked eye, can partially counter this problem (Davies, 2015). Cryptotephra analysis allows for the detection of much smaller tephra concentrations, revealing tephra at greater distances from volcanic sources (Wastegård et al., 1998; McKay et al., 2012). Volcanic glass shards within tephra layers are also prone to dissolution by laboratory processes (Blockley et al., 2005). Extraction of tephra shards through a stepped floatation protocol rather than by use of acid washing of sediments can limit the laboratory influences on tephra shards (Blockley et al., 2005). Comparison of multiple proximate cores can be used to correct for the local effects of dissolution (Abbott et al., 2018).

Tephra layers are prone to reworking, particularly by the tectonic forces that produce the tephra in the first place (Nakayama and Yoshikawa, 1997), leading to the development of inaccurate stratigraphies through misidentification of primary deposits (Hopkins et al., 2020). These problems can be partially overcome through analysis of many proximate sites (Abbott et al., 2018), and through modelling tephra reworking (Hopkins et al., 2020).

3 Project Structure

The three aims of the project are: 1) to characterise the change in ocean structure over the Pacific, 2) to determine the changes in AMOC strength, and 3) to detect any effects on the rates of volcanism, due to the iNHG. This section will look at the results that have already been obtained, the future experiments that are planned, and what likely results of these experiments would mean for these aims.

3.1 Ocean Structure in the Pacific

In the Late Pliocene Pacific Ocean there is a suggestion that there was an overturning circulation cell, the PMOC, which formed due to a weakened halocline in the subpolar North Pacific (Burls et al., 2017). This suggestion is controversial and not universally accepted (Zhang et al., 2021), and the structure of the deep Pacific Ocean during a PMOC is not well understood. Over the iNHG, the PMOC ceases, and there is a convergence in deep water mass properties in the Atlantic and Pacific Oceans (Woodard et al., 2014). This convergence implies that there was greater connectivity between the Atlantic and Pacific Oceans after the iNHG. This could be related to the shutdown in the PMOC, or could be due to greater deep water export from the Southern Ocean (Hill et al., 2017), or the North Atlantic (Kwiek and Ravelo, 1999).

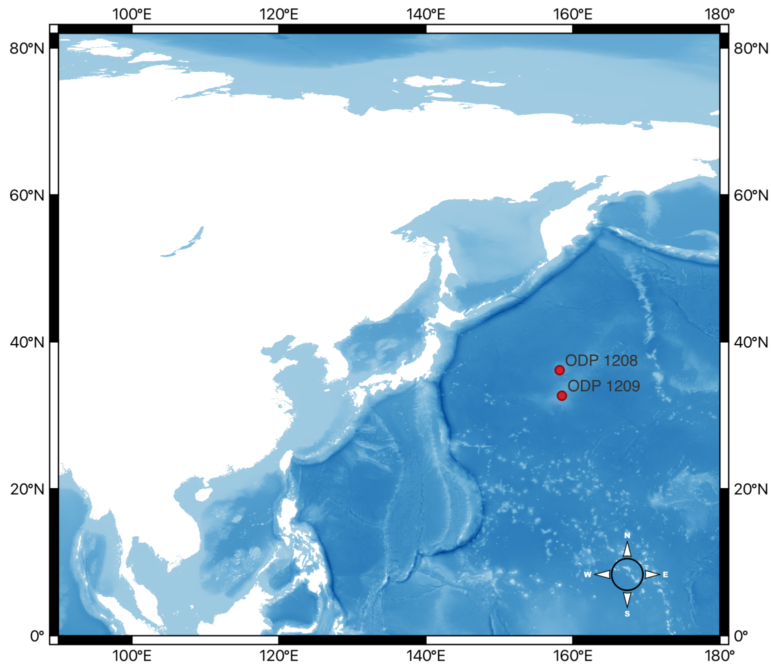

Figure 11: Map of the North West Pacific Ocean showing the location of ODP Sites 1208 and 1209. From GEBCO (2021)

The focus of this chapter of the project is to determine the physical characteristics of the intermediate and deep waters of the Pacific during the PMOC and after it has stopped. The project is looking at two sites in the North West Pacific Ocean, ODP Sites 1208 (3346 m depth) and 1209 (2387 m depth) (Bralower et al., 2002). Their location (figure 11) allows them to sample any deep waters that might form in the North Pacific which would then be carried southwards by deep western boundary currents (Fontela et al., 2020). The lack of Pacific deep water formation means that both sites are bathed in the same poorly ventilated, nutrient-rich, southern-sourced water mass in the present day. In the Late Pliocene, active deep water formation would have resulted in a relatively fresh, cold, well-ventilated NPDW extending to approximately 3000 m depth (figure 12) (Burls et al., 2017). It is expected that site 1209 would be bathed in this fresher NPDW while the deeper site 1208 would only sample AABW from the Southern Ocean.

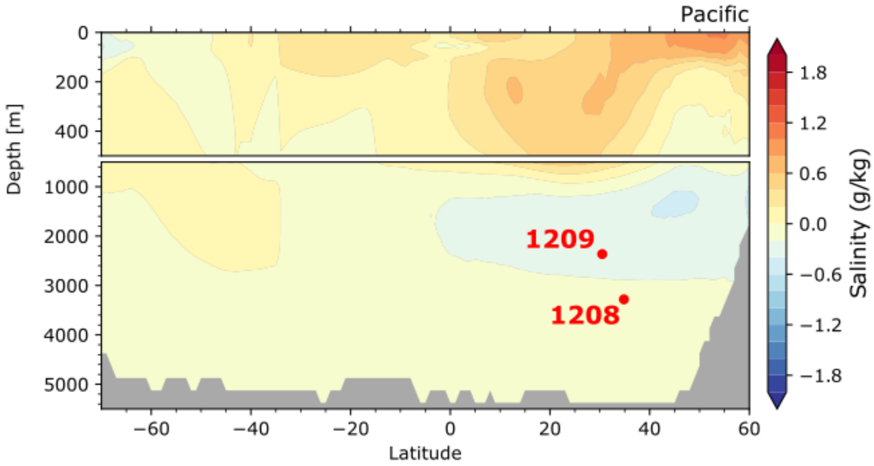

(a) Salinity

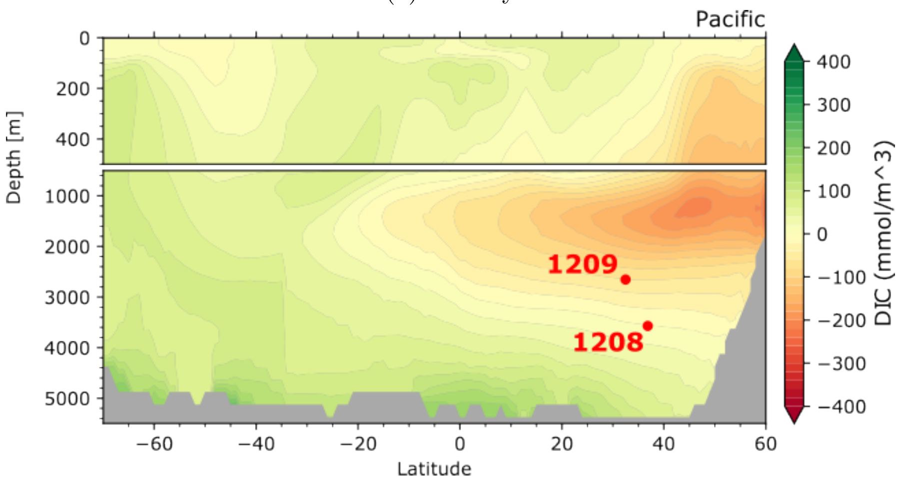

(b) DIC

Figure 12: Model output showing salinity and dissolved inorganic carbon, DIC, in the Pacific Ocean in the Late Pliocene relative to the preindustrial. From Ford et al. (2022)

3.1.1 Results and Discussion

Oxygen isotope measurements were made on *Cibicidoides wuellerstorfi* foraminifera from Site 1209 over the Late Pliocene and Early Pleistocene. There were compared to existing δ^{18}O records from the same time period from Site 1208 (Venti et al., 2017). Positive δ^{18}O values are usually associated with colder or more saline, and thus denser, water masses. In the Late Pliocene, more positive δ^{18}O values are seen at Site 1209 compared to 1208, despite 1209 being the shallower site (figure 13). This divergence in oxygen isotopes begins around 3.3 Ma and continues until the end fo the iNHG, around 2.5 Ma.

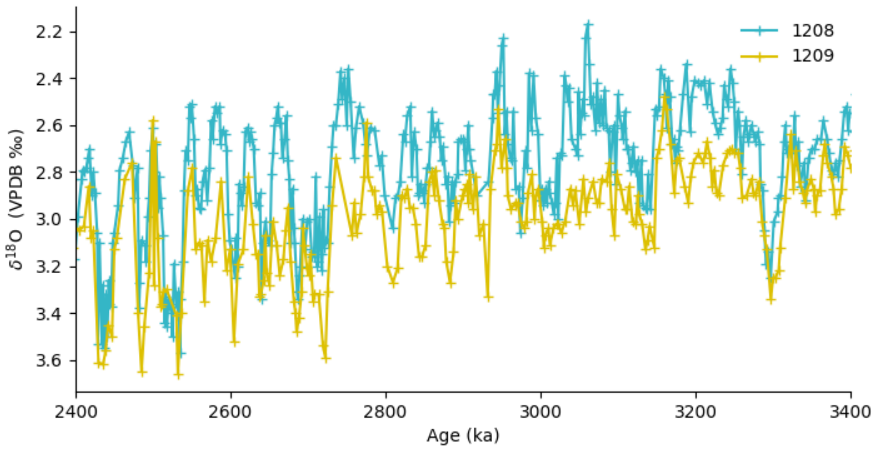

Figure 13: Oxygen isotope measurements from *Cibicidoides wuellerstorfi* from ODP Site 1208 (Venti et al., 2017) and 1209 (Ford, unpublished)

In the present day there is no major difference in oxygen isotope values between the two sites. The modern North Pacific is homogenous in oxygen isotopes, with the difference in intermediate and deep ocean δ^{18}O values being less than 0.465 ‰(95% confidence, figure 19). In the North and Southern Atlantic there is a greater heterogeneity between intermediate and deep waters, and the differences are generally less than 0.59‰and 0.72‰respectively (figure 19). This difference is driven by the deep water formation in the Atlantic which causes different water masses to overly one another. The difference in δ^{18}O regularly exceeds 0.6‰in the Late Pliocene, pointing to a different ocean structure in the Pliocene Pacific Ocean compared to the present.

The heavier oxygen isotopes at the shallower Site 1209 over Site 1208 requires a decoupling of δ^{18}O values and salinity. The formation of AABW off the coast of Antarctica is driven in part by brine-rejection from the formation of sea ice, which increases the salinity of these surface waters without fractionating any oxygen isotopes, and would result in more saline, denser waters, without a correspondingly heavier δ^{18}O signal. A similar process occurs in the modern South Atlantic Ocean (Lynch-Stieglitz et al., 2006). The greater δ^{18}O values at 1209 could be explained by NPDW at this site being colder, but fresher, than the underlying AABW (figure 12).

The δ^{18}O measurements from Sites 1208 and 1209 converge over the iNHG. This is likely due to the formation of a strong halocline in the North Pacific inhibiting NPDW formation. The oxygen isotope record converges more during glacials and less during interglacials indicating that the lower temperatures or greater ice volume of the Early Pleistocene may be responsible for suppressing NPDW formation.

Measurements of the Mg/Ca ratio were made of *Uvigerina peregrina* foraminifera from Site 1209 over the iNHG. These results were compared to a similar record from Site 1208 (Woodard et al., 2014), and both records were combined with δ^{18}O measurements in a bootstrap Monte Carlo model to solve for temperature and $\delta^{18}O_{sw}$ (figure 14) (Thirumalai et al., 2016).

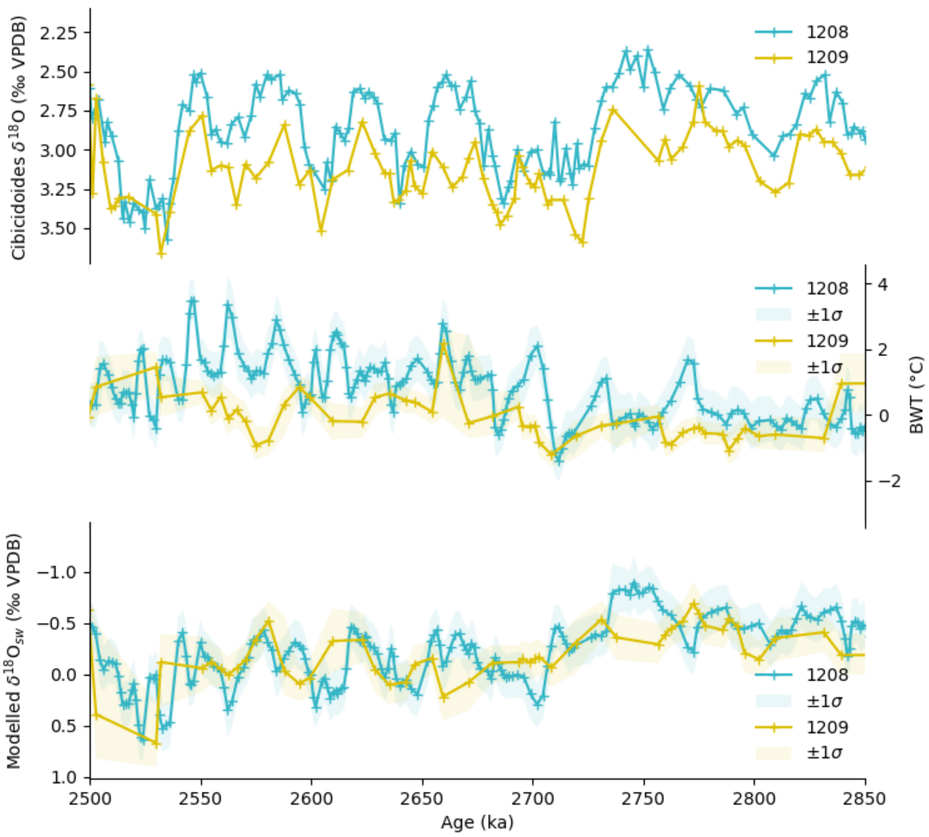

Figure 14: Comparison of Mg/Ca derived BWT and δ^{18}O estimates from Sites 1208 (Woodard et al., 2014; Venti et al., 2017) and 1209 (Ford, unpublished, and own work). Estimates of BWT and $\delta^{18}O_{sw}$ are generated using PSU Solver from Thirumalai et al. (2016)

The BWT estimates from Site 1209 show colder temperatures than at 1208 for much of the iNHG, with converging driven by a slight warming at Site 1209 in the Early Pleistocene. The $\delta^{18}O_{sw}$ estimates, a proxy for salinity, show similar values for both sites within error. These results support the idea that Site 1209 is being bathed in fresher, colder, NPDW from an active PMOC in the Late Pliocene. The convergence in $\delta^{18}O$ over the iNHG is driven by a warming at Site 1209, likely reflecting an increased influence of AABW at the site as the PMOC is shut down. The convergence of BWT over the iNHG is more pronounced during glacials, with cooling at 1208 during glacial periods, contrasting with the gradually rising BWT at Site 1209. The glacial-interglacial variability in BWT at Site 1208 supports the idea of growing Pleistocene ice sheets playing a role in cooling the Southern Ocean over the iNHG. This could have led to an increase in deep water formation, encouraging the export of CDW and AABW from the Southern Ocean into the Pacific Basin. The gradual warming in BWT at 1209 suggests that if there is a shutdown in NPDW formation over the iNHG, it is not an instantaneous process centred on 2.73 Ma but occurs more gradually.

The record of BWT from 1209 is much less variable than that at 1208, particularly on glacial-interglacial timescales in the Early Pleistocene. This could reflect the increasing influence of ice sheet and sea ice expansion on the southern-sourced AABW (Hill et al., 2017), or could be the result of the low resolution of the 1209 Mg/Ca record having aliasing issues.

North Atlantic BWT records from Site 607 (figure 15) also show a convergence with the BWT record at Site 1208, over a similar timescale to the convergence at Site 1209. DSDP Site 607 is located at 3426 m depth in the North Atlantic, and samples NADW exported from further North (Ruddiman et al., 1987). The BWT record at Site 607 shows a cooling over the iNHG, while the convergence at Site 1209 is driven by a warming in BWT. The opposite sign of temperature change at the two sites suggests that the convergence in North Pacific BWT is not driven by greater NADW import (Kwiek and Ravelo, 1999).

The convergence of the deep water mass properties at all three sites (figure 15) could indicate a common water mass bathing all three sites. This might be the result of stronger AABW and CDW export over the iNHG, due to an expansion in Antarctic sea ice, causing an increase homogeneity in Pacific and Atlantic water masses (Woodard et al., 2014).

3.1.2 Future Directions

The next aim of this project is to undertake more measurements of the Mg/Ca ratios on foraminifera at Site 1209. More measurements in the Early Pleistocene will allow me to resolve whether the convergence in $\delta^{18}O$ and Mg/Ca values is influenced by glacial-interglacial cycles. A higher resolution record could show that BWT at Site 1208 and 1209 converges more during glacials and then diverges during interglacials, suggesting a strong role for ice growth in modulating the PMOC shutdown. The final convergence of the $\delta^{18}O$ records at 2.55 Ma, coincident with evidence for marine-terminating ice sheets in the Gulf of Alaska (Maslin et al., 1996), suggests that ice sheet growth over the iNHG

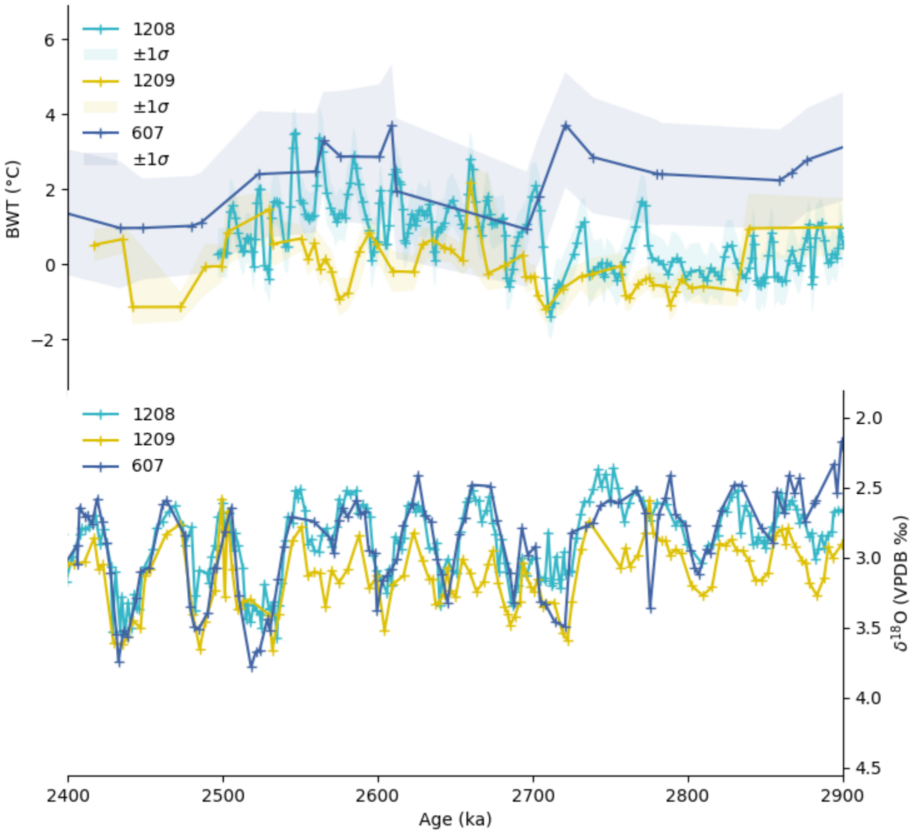

Figure 15: Comparison of Mg/Ca derived BWT estimates for Sites 1209, 1208 (Woodard et al., 2014) and 607 (Sosdian and Rosenthal, 2009)

may have played a role in establishing a North Pacific halocline.

Alternatively, a higher resolution BWT record could show the waters at Site 1209 becoming gradually warmer with no apparent orbital forcing. This would imply that atmospheric moisture transport is more likely the main driver of halocline formation over the iNHG (Burls et al., 2017). Increased meridional atmospheric moisture transport has been suggested as a factor in the initiation of the iNHG (Brierley and Fedorov, 2010) and could explain the synchronous timings of the PMOC shutdown and the iNHG.

Deep waters formed in the subpolar North Pacific would be more ventilated in the deep Pacific Ocean than those from the Southern Ocean (figure 12). The NPDW formed from an active PMOC will have a lower dissolved inorganic carbon, DIC, content, and thus higher $\left[CO_3^{2-}\right]$, than AABW. The difference in DIC can be seen in carbon isotopes

(Ford et al., 2022) and B/Ca measurements. The next steps are to undertake B/Ca measurements in *Cibicidoides wuellerstorfi* from Site 1209 to compare to existing measurements from Site 1208 (Rosenthal, unpublished). The B/Ca measurements will give an estimate of how $\left[CO_3^{2-}\right]$ values changed over the iNHG.

It is expected that the $\left[CO_3^{2-}\right]$ values would be higher at Site 1209 than 1208 during the Pliocene, reflecting the DIC-poor, well-ventilated NPDW bathing Site 1209 (figure 12). A similar structure is seen in the modern North Atlantic, where the well-ventilated NADW has a higher $\left[CO_3^{2-}\right]$ content than the underlying poorly ventilated AABW (Chalk et al., 2019).

The results could show similar $\left[CO_3^{2-}\right]$ values at both Site 1208 and 1209. This is similar to the situation in the modern Pacific Ocean where there is little heterogeneity in DIC content. This could therefore reflect the absence of a PMOC in the Late Pliocene. Equally, it could show that NPDW formation occurs in a nutrient-rich, upwelling environment, in contrast to NADW which forms from nutrient-limited surface waters (Skinner et al., 2020). The idea of a nutrient-rich NPDW is supported by high opal accumulation rates in the Late Pliocene subpolar North Pacific (Haug et al., 2005; Swann, 2010). If this were the case, it would imply that CO_2 storage of the deep Pacific was not hugely different in the Pliocene relative to the present. The Pacific Ocean is a major store of carbon (Cheng et al., 2017), and so this would suggest that the higher CO_2 levels of the Late Pliocene were not driven by Pacific Ocean changes (Bartoli et al., 2011).

The B/Ca measurements from Site 1209 may also indicate lower $\left[CO_3^{2-}\right]$ values than at 1208. If this were the case, it would suggest that the formation of deep waters in the Southern Ocean is likely different to today, with greater degassing and ventilation causing higher $\left[CO_3^{2-}\right]$ values in the Late Pliocene AABW.

3.2 Changes in AMOC Strength

The changes in AMOC strength over the iNHG are poorly understood, with evidence pointing to a stronger, weaker and unchanged overturning circulation during the iNHG (Raymo et al., 1992; Hayashi et al., 2020; Lang et al., 2016). The AMOC is a key driver of ocean circulation (Talley et al., 2011) and has major impacts on ocean structure in the Pacific and Atlantic basins.

The strength of the AMOC overturning is usually derived from proxies for the spatial extent of NADW, with a greater extent of NADW implying a stronger AMOC. However, the extent of NADW is dependent on AMOC strength but also the export of water masses in the Southern Ocean. There are many studies from the North (Hayashi et al., 2020; Lang et al., 2016) and South (Hodell and Venz, 1992; Raymo et al., 1992) Atlantic over the iNHG but few from the mid-Atlantic where the extent of NADW could be most clearly seen. This project will reconstruct the BWT, $\left[CO_3^{2-}\right]$ and ε_{Nd} in the Central Atlantic to characterise and understand the spatial extent of northern and southern-sourced deep waters. This will allow us to better constrain the spatial extent of the NADW in the mid-Atlantic over the iNHG and infer how AMOC strength may have changed.

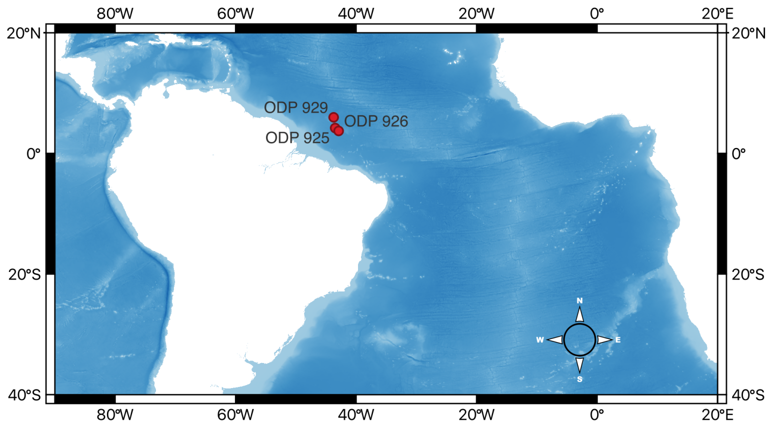

Figure 16: Map of the Central Ocean showing the location of ODP Sites 925, 926 and 929. From GEBCO (2021)

This study will look at ODP Sites 925, 296 and 929 in the Central Atlantic (figure 16). These sites are located on the Ceara Rise, off the coast of Brazil, at depths of 3042 m, 3609 m, and 4369 m depth respectively (Curry et al., 1995). The modern day boundary between AABW and NADW in the Central Atlantic sits around 4000 m depth (Curry et al., 1995), and so these sites are well suited to determining how this boundary has changed over time in response to circulation strength.

The first aim of this project will be to generate an Mg/Ca record for the three sites. This record will focus on the Late Pliocene interglacial KM5c (c. 3.205 Ma) and the Early Pleistocene glacials and interglacial MIS 100 and 99 (2.50 - 2.52 Ma) (figure 17). These periods, before and after the iNHG, will allow for a good reconstruction of the changes that occurred over this transition. The results from interglacial KM5c can be compared with the results from the PlioVAR data synthesis project (McClymont et al., 2020), and the PlioMIP model intercomparison project (Haywood et al., 2020), which both focus on this interval. This interglacial is thought to be representative of a "normal" Late Pliocene climate state. In the Early Pleistocene there are several records from the North Atlantic which cover MIS 100 and 99 (Ohno et al., 2016; Groeneveld et al., 2014) allowing for detailed comparison.

The Mg/Ca record from these sites will be used to determine how BWT changed across a depth-transect of the Central Atlantic Ocean over the iNHG. These results will be compared to existing $\delta^{18}O$ measurements from the sites (figure 17) (Wilkens et al., 2017) to estimate how $\delta^{18}O_{sw}$ may have changed. The existing records show a convergence in $\delta^{18}O$ between Sites 929 and 925 from the Late Pliocene to the Early Pleistocene (figure 17). The Mg/Ca results from before and after the iNHG should help to deconvolve why this convergence occurred.

The BWT record at Sites 925 and 926 could show a cooling, converging with the expected colder temperatures at Site 929. This would match what is seen at Site 607

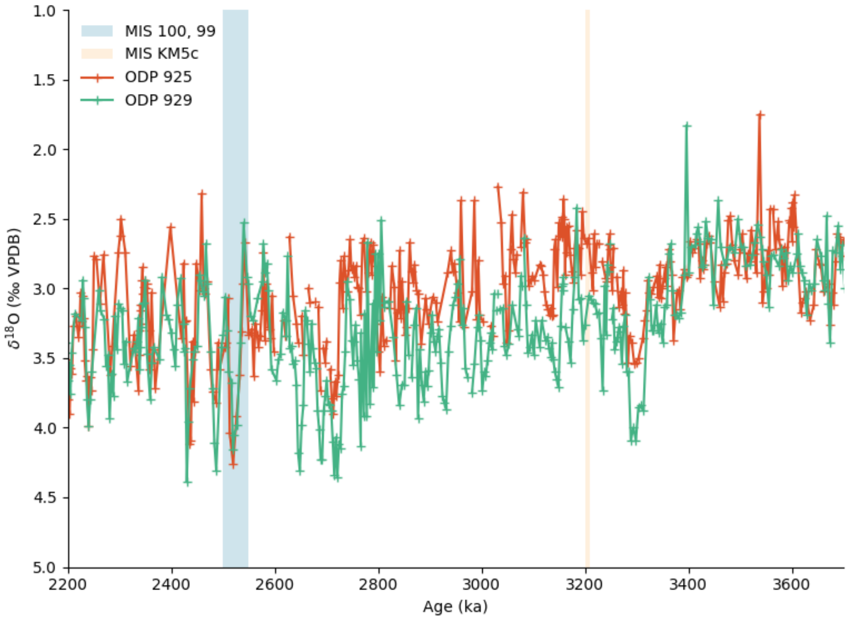

Figure 17: δ^{18}O records from the intermediate (Site 925) and deep (Site 929) Central Atlantic Ocean over the iNHG. Shaded regions show MIS KM5c (3.21 - 3.22 Ma) and MIS 100, 99 (2.50 - 2.52 Ma). Data from Wilkens et al. (2017)

over the iNHG (Sosdian and Rosenthal, 2009; Woodard et al., 2014) with a cooling in NADW temperatures to match the BWT from southern-sourced waters. This result would imply that there is a greater "Antarctic" influence on waters in the deep Atlantic, either due to an increase in CDW export or a decrease in AMOC strength over the iNHG.

Alternatively, the Mg/Ca measurements may show very little change in BWT over the iNHG, which would indicate that the convergence in δ^{18}O between Sites 925 and 929 (figure 17) is driven by salinity changes rather than temperature changes. This would be a different pattern to what is seen in the North Pacific but could be driven by an increase in salinity in the North Atlantic. An increase in salinity in the North Atlantic coincident with a freshening in the North Pacific suppressing NPDW formation would imply a strong salt transport from the Pacific to the Atlantic over the iNHG (Woodard et al., 2014).

An issue to consider is whether the convergence in δ^{18}O between Sites 925 and 929 over the iNHG is driven by a change in water mass properties or due to all the sites being bathed in the same water mass. The second part of the project will undertake B/Ca measurements on benthic foraminifera from the three sites, 925, 926 and 929, over the same intervals before and after the iNHG.

AABW forms in a nutrient-rich upwelling zone in the Southern Ocean and so will have a lower $\left[CO_3^{2-}\right]$ content than NADW which forms in nutrient-limited subpolar North Atlantic. The B/Ca measurements can be used as a water mass tracer to infer which water mass is bathing which site.

A decrease in $\left[CO_3^{2-}\right]$ content over the iNHG at the shallower Site 925 could suggest that the site is being bathed in southern-sourced deep waters (Lang et al., 2016). This would point to a weaker AMOC or a stronger Southern Ocean deep water export over the iNHG. Alternatively, lower $\left[CO_3^{2-}\right]$ values could imply that there is a change in the ventilation structure of the deep North Atlantic. This could come about through an increased influence of poorly-ventilated, $\left[CO_3^{2-}\right]$-poor Nordic Seas waters into the NADW, as has been suggested for the Last Glacial (Larkin et al., 2022). However, other indicators for the North Atlantic do not suggest that there was a major change in ventilation patterns over the iNHG (Draut et al., 2003).

Alternatively, if there was little change in the $\left[CO_3^{2-}\right]$ values measured at the three sites over the iNHG, this would imply that the structure of the deep Central Atlantic Ocean did not change over the iNHG. This would mean that the convergence in $\delta^{18}O$ values is driven by a change in water mass properties, either in the North Atlantic or the Southern Ocean.

A change in $\left[CO_3^{2-}\right]$ values at a site could be the result of a change in nutrient utilisation or ventilation of water masses, or it could be the result of a change in the water mass bathing that site. The project will follow up with ε_{Nd} measurements at the three sites over the study intervals to determine the provenance of the particular water masses at each site. It is expected that, similar to today, NADW sourced from surface waters in the North Atlantic will have much more negative ε_{Nd} values than waters sourced from the Southern Ocean (van de Flierdt et al., 2016).

The end-member compositions of either NADW or AABW may be different in the Late Pliocene or Early Pleistocene compared to the present. Comparison with other ε_{Nd} records from the Pliocene North Atlantic (Lang et al., 2016) will help to constrain the ε_{Nd} signal of NADW which will allow for better reconstructions of water mass provenance.

3.3 Effects on Volcanism

The final chapter of this project will look at how volcanism may have changed in response to the iNHG. Volcanism is a major driver of past climatic change (McKenzie et al., 2016) and so understanding the drivers of volcanism is key to understanding past climates.

The aim of this chapter of the project is to construct a record of volcanism on Iceland for the Late Pliocene and Early Pleistocene from tephra in marine sediments cores, and to determine if there is a significant change in the rate of volcanism over the iNHG on Iceland. The most effective method of inferring changes in the strength of volcanism over the iNHG is to look at marine tephra records from the Late Pliocene. Tephra records provide the most accessible way of inferring past rates of volcanism and marine cores are the only locations where these sediments are preserved over this time period (Cassidy et al., 2014).

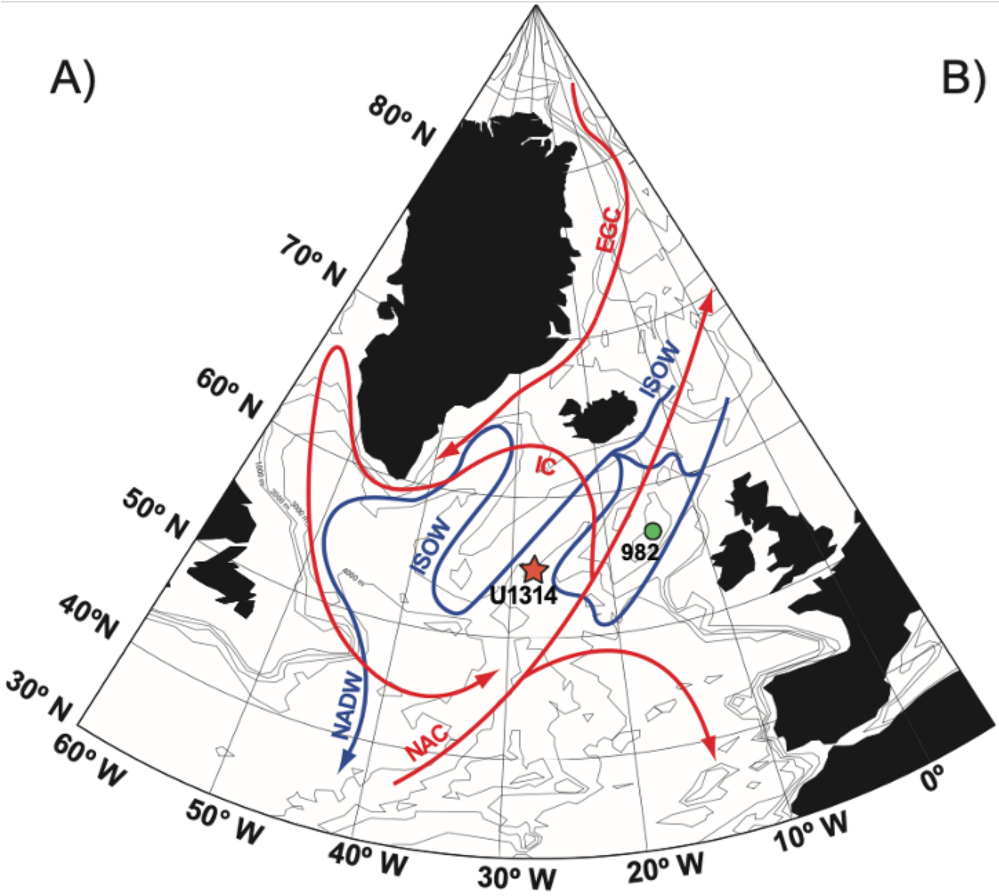

Figure 18: The location of U1314 in the Northeast Atlantic Ocean showing also the ODP Site 982 and the location of major deep (blue) and surface (red) ocean currents. From Hernández-Almeida et al. (2014)

The first part of this chapter will look at tephra layers at IODP Site U1314 in the North East Atlantic Ocean (figure 18). This site is located directly south of Iceland, on the Gardar Drift, and so will be able to sample tephra ejected from Icelandic volcanism. There is reasonable tephra preservation at the site for the last glacial (Abbott et al., 2018), though typically tephra from Iceland volcanism is carried to the southeast (Davies et al., 2010). Initial studies have noted the presence of tephra in Pliocene sections of U1314 (Channell et al., 2016). If there are sufficiently high tephra counts at the site, the relative change in tephra deposition before and after the iNHG could be used to infer the rate of volcanism over the transition.

There exists a magnetostratigraphic age model for the Site U1314 for the Early Pleistocene (Ohno et al., 2012), but not for the Late Pliocene. Therefore, this project will measure the δ^{18}O of benthic foraminifera to tie these measurements to the global ProbStack oxygen isotope record (Ahn et al., 2017). From these tie points, the aim is to make an age model for the Late Pliocene at Site U1314.

If there is a reliable tephra record at U1314, a tephra record will be generated for ODP Site 982 over the same period (figure 18). There already exists an age model for Site 982 covering the iNHG (Khélifi et al., 2012). A greater spatial extent of tephra records over the iNHG will add strength to any conclusions about the rate of volcanism over the iNHG. These two records are from far enough apart in the Northeast Atlantic Ocean that local factors, such as dissolution or ice-rafting of tephra, are unlikely to have a major impact on conclusions drawn from the two records.

If there is a decrease in tephra layers then this will likely be the result of increased ice loading on Iceland causing an increase in subsurface pressure. This increase in pressure will decrease the degree of magmatic melting which is linked to volcanism (Schmidt et al., 2013; Maclennan et al., 2002).

If there is an increase in tephra layers over the iNHG, this would suggest that the rate of volcanism increased on Iceland over the iNHG. This may be due to fracturing of the crust with the advance and retreat of ice sheets in the Early Pleistocene allowing more pathways for magma to rise to the surface (Jellinek et al., 2004).

There may be insufficient tephra at Site U1314 to draw any conclusions about the changes in volcanism over the iNHG. In this case, the δ^{18}O record from Site U1314 will be augmented with Mg/Ca measurements on benthic foraminifera from Site U1314 from before and after the iNHG. The coupled BWT and $\delta^{18}O_{sw}$ estimates will allow for a better understanding of how NADW changed over the iNHG. Site U1314 is bathed in Iceland-Scotland Overflow Water (ISOW), a major component of NADW that is formed from cold surface waters in the Arctic and Nordic Seas (Xu et al., 2018). If this record shows a cooling in BWT over the iNHG, akin to what is seen at Site 607 (Sosdian and Rosenthal, 2009), then this would suggest that the convergence in deep water properties over the iNHG between the Atlantic and Pacific Oceans is driven by a cooling in NADW (Woodard et al., 2014) rather than an increased influence of AABW, which is unlikely to influence deep waters this far north.

A Appendix

A.1 GANTT Chart

Below is a GANTT Chart describing the idealised progression of the project over the next three years in order to complete the PhD project by September 2025.

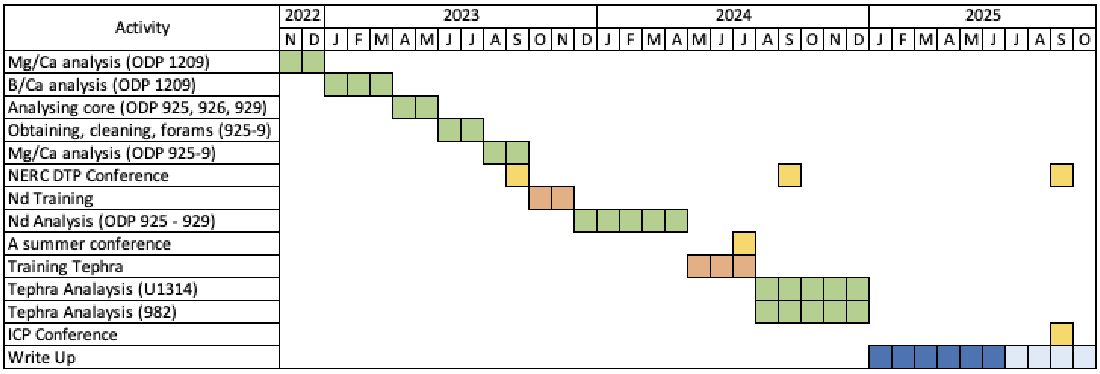

A.2 Homogeneity of the Pacific Ocean

The modern Pacific Ocean is relatively homogenous in $\delta^{18}O$ space. This can be seen by looking at the difference in oxygen isotopes between intermediate waters (defined as being lower than 2000 m depth) and deep waters (defined as being at at least 2500 m depth) in the North Pacific Ocean relative to other ocean basins (figure 19). The data come from core-top $\delta^{18}O$ measurements from (Schmittner et al., 2017).

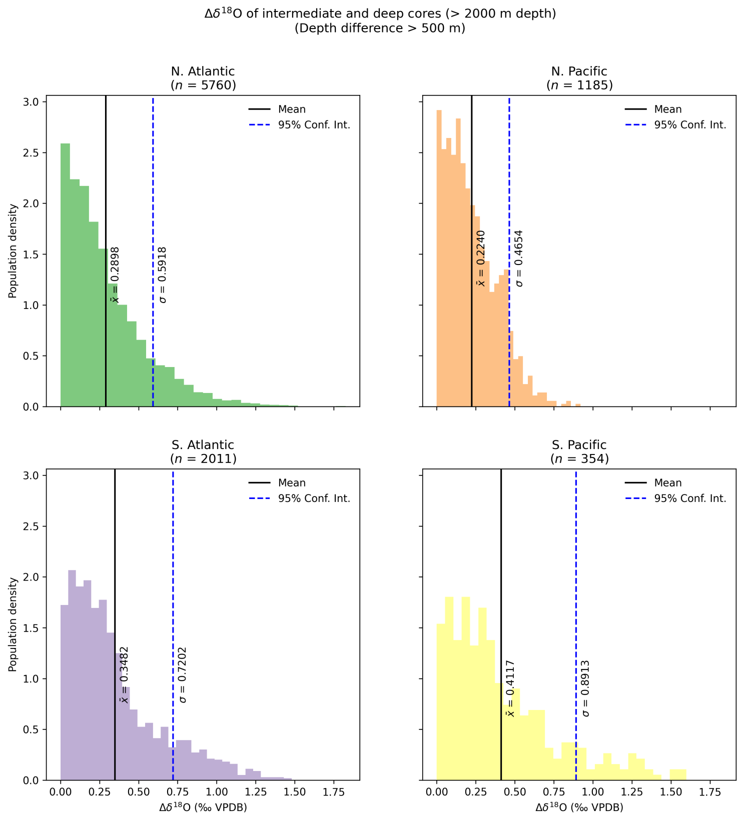

Figure 19: Histograms showing the difference in modern $\delta^{18}O$ measurements from core tops sampling intermediate (between 2000 - 2500 m depth) and deep (below 2500 m depth) for various ocean basins. Data from Schmittner et al. (2017)]

References

Abbott, A. N., Haley, B. A., and McManus, J. (2015). Bottoms up: Sedimentary control of the deep North Pacific Ocean's eNd signature. *Geology*, 43(11):1035.

Abbott, P. M., Griggs, A. J., Bourne, A. J., and Davies, S. M. (2018). Tracing marine cryptotephras in the North Atlantic during the last glacial period: Protocols for identification, characterisation and evaluating depositional controls. *Marine Geology*, 401:81–97.

Ahn, S., Khider, D., Lisiecki, L. E., and Lawrence, C. E. (2017). A probabilistic Pliocene–Pleistocene stack of benthic 18O using a profile hidden Markov model. *Dynamics and Statistics of the Climate System*, 2(1).

Amakawa, H., Nozaki, Y., Alibo, D. S., Zhang, J., Fukugawa, K., and Nagai, H. (2004). Neodymium isotopic variations in Northwest Pacific waters. *Geochimica et Cosmochimica Acta*, 68(4):715–727.

Aubry, T. J., Farquharson, J. I., Rowell, C. R., Watt, S. F. L., Pinel, V., Beckett, F., Fasullo, J., Hopcroft, P. O., Pyle, D. M., Schmidt, A., and Sykes, J. S. (2022). Impact of climate change on volcanic processes: current understanding and future challenges. *Bulletin of Volcanology*, 84(6):58.

Badger, M. P. S., Schmidt, D. N., Mackensen, A., and Pancost, R. D. (2013). High-resolution alkenone palaeobarometry indicates relatively stable pCO2 during the Pliocene (3.3-2.8 Ma). *Philosophical Transactions: Mathematical, Physical and Engineering Sciences*, 371(2001):1–16. Publisher: The Royal Society.

Bailey, I., Hole, G. M., Foster, G. L., Wilson, P. A., Storey, C. D., Trueman, C. N., and Raymo, M. E. (2013). An alternative suggestion for the Pliocene onset of major northern hemisphere glaciation based on the geochemical provenance of North Atlantic Ocean ice-rafted debris. *Quaternary Science Reviews*, 75:181–194.

Barker, S., Greaves, M., and Elderfield, H. (2003). A study of cleaning procedures used for foraminiferal Mg/Ca paleothermometry. *Geochemistry, Geophysics, Geosystems*, 4(9). _eprint: https://onlinelibrary.wiley.com/doi/pdf/10.1029/2003GC000559.

Barrientos, N., Lear, C. H., Jakobsson, M., Stranne, C., O'Regan, M., Cronin, T. M., Gukov, A. Y., and Coxall, H. K. (2018). Arctic Ocean benthic foraminifera Mg/Ca ratios and global Mg/Ca-temperature calibrations: New constraints at low temperatures. *Geochimica et Cosmochimica Acta*, 236:240–259.

Bartoli, G., Hönisch, B., and Zeebe, R. E. (2011). Atmospheric CO_2 decline during the Pliocene intensification of Northern Hemisphere glaciations. *Paleoceanography*, 26(4). _eprint: https://onlinelibrary.wiley.com/doi/pdf/10.1029/2010PA002055.

Bartoli, G., Sarnthein, M., Weinelt, M., Erlenkeuser, H., Garbe-Schönberg, D., and Lea, D. (2005). Final closure of Panama and the onset of northern hemisphere glaciation. *Earth and Planetary Science Letters*, 237(1-2):33–44.

Batchelor, C. L., Margold, M., Krapp, M., Murton, D. K., Dalton, A. S., Gibbard, P. L., Stokes, C. R., Murton, J. B., and Manica, A. (2019). The configuration of Northern Hemisphere ice sheets through the Quaternary. *Nature Communications*, 10(1):3713.

Bentov, S. and Erez, J. (2006). Impact of biomineralization processes on the Mg content of foraminiferal shells: A biological perspective. *Geochemistry, Geophysics, Geosystems*, 7(1). _eprint: https://onlinelibrary.wiley.com/doi/pdf/10.1029/2005GC001015.

Benway, H. M. and Mix, A. C. (2004). Oxygen isotopes, upper-ocean salinity, and precipitation sources in the eastern tropical Pacific. *Earth and Planetary Science Letters*, 224(3-4):493–507.

Bizimis, M. and Scher, H. D. (2016). Neodymium Isotopes. In Bobrowsky, P. and Marker, B., editors, *Encyclopedia of Engineering Geology*, pages 1–6. Springer International Publishing, Cham. Series Title: Encyclopedia of Earth Sciences Series.

Blockley, S., Pyne-O'Donnell, S., Lowe, J., Matthews, I., Stone, A., Pollard, A., Turney, C., and Molyneux, E. (2005). A new and less destructive laboratory procedure for the physical separation of distal glass tephra shards from sediments. *Quaternary Science Reviews*, 24(16-17):1952–1960.

Boulahanis, B., Carbotte, S. M., Huybers, P. J., Nedimović, M. R., Aghaei, O., Canales, J. P., and Langmuir, C. H. (2020). Do sea level variations influence mid-ocean ridge magma supply? A test using crustal thickness and bathymetry data from the East Pacific Rise. *Earth and Planetary Science Letters*, 535:116121.

Bourne, A., Cook, E., Abbott, P., Seierstad, I., Steffensen, J., Svensson, A., Fischer, H., Schüpbach, S., and Davies, S. (2015). A tephra lattice for Greenland and a reconstruction of volcanic events spanning 25–45 ka b2k. *Quaternary Science Reviews*, 118:122–141.

Boyle, E. and Keigwin, L. (1985). Comparison of Atlantic and Pacific paleochemical records for the last 215,000 years: changes in deep ocean circulation and chemical inventories. *Earth and Planetary Science Letters*, 76(1-2):135–150.

Bralower, T., Premoli Silva, I., Malone, M., Arthur, M., Averyt, K., and Bown, P. (2002). Leg 198 Summary. In *Proceedings of the Ocean Drilling Program, 198 Initial Reports*, volume 198 of *Proceedings of the Ocean Drilling Program*. Ocean Drilling Program.

Branson, O., Redfern, S. A., Tyliszczak, T., Sadekov, A., Langer, G., Kimoto, K., and Elderfield, H. (2013). The coordination of Mg in foraminiferal calcite. *Earth and Planetary Science Letters*, 383:134–141.

Brierley, C. M. and Fedorov, A. V. (2010). Relative importance of meridional and zonal sea surface temperature gradients for the onset of the ice ages and Pliocene-Pleistocene climate evolution: SST GRADIENTS AND ICE AGES. *Paleoceanography*, 25(2).

Brierley, C. M. and Fedorov, A. V. (2016). Comparing the impacts of Miocene–Pliocene changes in inter-ocean gateways on climate: Central American Seaway, Bering Strait, and Indonesia. *Earth and Planetary Science Letters*, 444:116–130.

Broecker, W., Bond, G., Klas, M., Clark, E., and McManus, J. (1992). Origin of the northern Atlantic's Heinrich events. *Climate Dynamics*, 6(3-4):265–273.

Brown, E., Colling, A., Park, D., Phillips, J., Rothery, D., and Wright, J. (2001). Chapter 2 - The atmosphere and the ocean. In Brown, E., Colling, A., Park, D., Phillips, J., Rothery, D., and Wright, J., editors, *Ocean Circulation (Second Edition)*, pages 17–36. Butterworth-Heinemann, Oxford.

Brown, S. J. and Elderfield, H. (1996). Variations in Mg/Ca and Sr/Ca ratios of planktonic foraminifera caused by postdepositional dissolution: Evidence of shallow Mg-dependent dissolution. *Paleoceanography*, 11(5):543–551.

Burls, N. J. and Fedorov, A. V. (2014). Simulating Pliocene warmth and a permanent El Niño-like state: The role of cloud albedo. *Paleoceanography*, 29(10):893–910.

Burls, N. J., Fedorov, A. V., Sigman, D. M., Jaccard, S. L., Tiedemann, R., and Haug, G. H. (2017). Active Pacific meridional overturning circulation (PMOC) during the warm Pliocene. *Science Advances*, 3(9):e1700156.

Cassidy, M., Watt, S. F., Palmer, M. R., Trofimovs, J., Symons, W., Maclachlan, S. E., and Stinton, A. J. (2014). Construction of volcanic records from marine sediment cores: A review and case study (Montserrat, West Indies). *Earth-Science Reviews*, 138:137–155.

Chalk, T., Foster, G., and Wilson, P. (2019). Dynamic storage of glacial CO2 in the Atlantic Ocean revealed by boron co3 and ph records. *Earth and Planetary Science Letters*, 510:1–11.

Channell, J. E. T., Harrison, R. J., Lascu, I., McCave, I. N., Hibbert, F. D., and Austin, W. E. N. (2016). Magnetic record of deglaciation using FORC-PCA, sortable-silt grain size, and magnetic excursion at 26 ka, from the Rockall Trough (NE Atlantic): A MAGNETIC RECORD OF DEGLACIATION. *Geochemistry, Geophysics, Geosystems*, 17(5):1823–1841.

Cheng, L., Trenberth, K. E., Fasullo, J., Boyer, T., Abraham, J., and Zhu, J. (2017). Improved estimates of ocean heat content from 1960 to 2015. *Science Advances*, 3(3):e1601545.

Conroy, J. L., Cobb, K. M., Lynch-Stieglitz, J., and Polissar, P. J. (2014). Constraints on the salinity–oxygen isotope relationship in the central tropical Pacific Ocean. *Marine Chemistry*, 161:26–33.

Criss, R. E. (1999). *Principles of Stable Isotope Distribution.* Oxford University Press, Incorporated, Cary, UNITED STATES.

Crocket, K., Vance, D., Gutjahr, M., Foster, G., and Richards, D. (2011). Persistent Nordic deep-water overflow to the glacial North Atlantic. *Geology*, 39(6):515–518.

Crumpton-Banks, J. and Rae, J. (2020). Boron Isotopes Provide Insights into Biomineralization, Seawater pH, and Ancient Atmospheric CO2. *Oceanography*, 33(2).

Curry, W., Shackleton, N., Richter, C., and et al., editors (1995). *Proceedings of the Ocean Drilling Program, 154 Initial Reports*, volume 154 of *Proceedings of the Ocean Drilling Program*. Ocean Drilling Program.

Davies, S. M. (2015). Cryptotephras: the revolution in correlation and precision dating. *Journal of Quaternary Science*, 30(2):114–130. _eprint: https://onlinelibrary.wiley.com/doi/pdf/10.1002/jqs.2766.

Davies, S. M., Larsen, G., Wastegård, S., Turney, C. S. M., Hall, V. A., Coyle, L., and Thordarson, T. (2010). Widespread dispersal of Icelandic tephra: how does the Eyjafjöll eruption of 2010 compare to past Icelandic events? *Journal of Quaternary Science*, 25(5):605–611. _eprint: https://onlinelibrary.wiley.com/doi/pdf/10.1002/jqs.1421.

Dean, W. E., Gardner, J. V., and Piper, D. Z. (1997). Inorganic geochemical indicators of glacial-interglacial changes in productivity and anoxia on the California continental margin. *Geochimica et Cosmochimica Acta*, 61(21):4507–4518.

Dissard, D., Nehrke, G., Reichart, G. J., and Bijma, J. (2010). The impact of salinity on the Mg/Ca and Sr/Ca ratio in the benthic foraminifera Ammonia tepida: Results from culture experiments. *Geochimica et Cosmochimica Acta*, 74(3):928–940.

Dokken, T. M. and Jansen, E. (1999). Rapid changes in the mechanism of ocean convection during the last glacial period. *Nature*, 401(6752):458–461. Number: 6752 Publisher: Nature Publishing Group.

Draut, A. E., Raymo, M. E., McManus, J. F., and Oppo, D. W. (2003). Climate stability during the Pliocene warm period. *Paleoceanography*, 18(4). _eprint: https://agupubs.onlinelibrary.wiley.com/doi/pdf/10.1029/2003PA000889.

Driscoll, N. W. and Haug, G. H. (1998). A Short Circuit in Thermohaline Circulation: A Cause for Northern Hemisphere Glaciation? *Science*, 282(5388):436–438. Publisher: American Association for the Advancement of Science.

Du, J., Haley, B. A., and Mix, A. C. (2016). Neodymium isotopes in authigenic phases, bottom waters and detrital sediments in the Gulf of Alaska and their implications for paleo-circulation reconstruction. *Geochimica et Cosmochimica Acta*, 193:14–35.

Elderfield, H., Ferretti, P., Greaves, M., Crowhurst, S., McCave, I. N., Hodell, D., and Piotrowski, A. M. (2012). Evolution of Ocean Temperature and Ice Volume Through the Mid-Pleistocene Climate Transition. *Science*, 337(6095):704–709. Publisher: American Association for the Advancement of Science Section: Research Article.

Elderfield, H., Yu, J., Anand, P., Kiefer, T., and Nyland, B. (2006). Calibrations for benthic foraminiferal Mg/Ca paleothermometry and the carbonate ion hypothesis. *Earth and Planetary Science Letters*, 250(3-4):633–649.

Eldrett, J. S., Harding, I. C., Wilson, P. A., Butler, E., and Roberts, A. P. (2007). Continental ice in Greenland during the Eocene and Oligocene. *Nature*, 446(7132):176–179. Number: 7132 Publisher: Nature Publishing Group.

Elstnerová, P., Friák, M., Fabritius, H. O., Lymperakis, L., Hickel, T., Petrov, M., Nikolov, S., Raabe, D., Ziegler, A., Hild, S., and Neugebauer, J. (2010). Ab initio study of thermodynamic, structural, and elastic properties of Mg-substituted crystalline calcite. *Acta Biomaterialia*, 6(12):4506–4512.

Emile-Geay, J. (2003). Warren revisited: Atmospheric freshwater fluxes and “Why is no deep water formed in the North Pacific”. *Journal of Geophysical Research*, 108(C6):3178.

Emiliani, C. (1955). Mineralogical and Chemical Composition of the Tests of Certain Pelagic Foraminifera. *Micropaleontology*, 1(4):377–380. Publisher: The Micropaleontology Project, Inc.

Erez, J. (2003). The Source of Ions for Biomineralization in Foraminifera and Their Implications for Paleoceanographic Proxies. In Dove, P. M., De Yoreo, J. J., and Weiner, S., editors, *Biomineralization*. De Gruyter.

Evans, D., Brierley, C., Raymo, M. E., Erez, J., and Müller, W. (2016). Planktic foraminifera shell chemistry response to seawater chemistry: Pliocene–Pleistocene seawater Mg/Ca, temperature and sea level change. *Earth and Planetary Science Letters*, 438:139–148.

Fedorov, A. V., Burls, N. J., Lawrence, K. T., and Peterson, L. C. (2015). Tightly linked zonal and meridional sea surface temperature gradients over the past five million years. *Nature Geoscience*, 8(12):975–980.

Ferreira, D., Cessi, P., Coxall, H. K., de Boer, A., Dijkstra, H. A., Drijfhout, S. S., Eldevik, T., Harnik, N., McManus, J. F., Marshall, D. P., Nilsson, J., Roquet, F., Schneider, T., and Wills, R. C. (2018). Atlantic-Pacific Asymmetry in Deep Water Formation. *Annual Review of Earth and Planetary Sciences*, 46(1):327–352.

Flower, B. P., Hastings, D. W., Hill, H. W., and Quinn, T. M. (2004). Phasing of deglacial warming and Laurentide Ice Sheet meltwater in the Gulf of Mexico. *Geology*, 32(7):597–600.

Fontela, M., Pérez, F. F., Mercier, H., and Lherminier, P. (2020). North Atlantic Western Boundary Currents Are Intense Dissolved Organic Carbon Streams. *Frontiers in Marine Science*, 7:593757.

Ford, H. L., Burls, N. J., Jacobs, P., Jahn, A., Caballero-Gill, R. P., Hodell, D. A., and Fedorov, A. V. (2022). Sustained mid-Pliocene warmth led to deep water formation in the North Pacific. *Nature Geoscience*, 15(8):658–663.

Foster, G. (2008). Seawater ph, pco2 and co3 variations in the Caribbean Sea over the last 130 kyr: A boron isotope and B/Ca study of planktic foraminifera. *Earth and Planetary Science Letters*, 271(1-4):254–266.

Frenz, M., Henrich, R., and Zychla, B. (2006). Carbonate preservation patterns at the Ceará Rise – Evidence for the Pliocene super conveyor. *Marine Geology*, 232(3):173–180.

Furue, R. and Endoh, M. (2005). Effects of the Pacific Diapycnal Mixing and Wind Stress on the Global and Pacific Meridional Overturning Circulation*. *Journal of Physical Oceanography*, 35(10):1876–1890.

Gebbie, G. and Huybers, P. (2006). Meridional circulation during the Last Glacial Maximum explored through a combination of South Atlantic d18O observations and a geostrophic inverse model. *Geochemistry, Geophysics, Geosystems*, 7(11). _eprint: https://onlinelibrary.wiley.com/doi/pdf/10.1029/2006GC001383.

Gebbie, G. and Huybers, P. (2011). How is the ocean filled? *Geophysical Research Letters*, 38(6). _eprint: https://onlinelibrary.wiley.com/doi/pdf/10.1029/2011GL046769.

GEBCO (2021). The GEBCO_2021 Grid - a continuous terrain model of the global oceans and land. *NERC EDS British Oceanographic Data Centre NOC*. Medium: Documents,Network Common Data Form Version Number: 1 Type: dataset.

Geirsdóttir, Á. and Eiríksson, J. (1994). Growth of an Intermittent Ice Sheet in Iceland during the Late Pliocene and Early Pleistocene. *Quaternary Research*, 42(2):115–130. Publisher: Cambridge University Press.

Gladenkov, A. Y., Oleinik, A. E., Marincovich, L., and Barinov, K. B. (2002). A refined age for the earliest opening of Bering Strait. *Palaeogeography, Palaeoclimatology, Palaeoecology*, 183(3):321–328.

Glazner, A. F., Manley, C. R., Marron, J. S., and Rojstaczer, S. (1999). Fire or ice: anticorrelation of volcanism and glaciation in California over the past 800,000 years. *Geophysical Research Letters*, 26(12):1759–1762. _eprint: https://onlinelibrary.wiley.com/doi/pdf/10.1029/1999GL900333.

Goldstein, S. and Hemming, S. (2003). Long-lived Isotopic Tracers in Oceanography, Paleoceanography, and Ice-sheet Dynamics. In *Treatise on Geochemistry*, pages 453–489. Elsevier.

Gonfiantini, R., Wassenaar, L. I., and Araguas-Araguas, L. J. (2020). Stable isotope fractionations in the evaporation of water: The wind effect. *Hydrological Processes*, 34(16):3596–3607.

Gray, W. R. and Evans, D. (2019). Nonthermal Influences on Mg/Ca in Planktonic Foraminifera: A Review of Culture Studies and Application to the Last Glacial Maximum. *Paleoceanography and Paleoclimatology*, 34(3):306–315.

Groeneveld, J., Hathorne, E., Steinke, S., DeBey, H., Mackensen, A., and Tiedemann, R. (2014). Glacial induced closure of the Panamanian Gateway during Marine Isotope Stages (MIS) 95–100 (c. 2.5 Ma). *Earth and Planetary Science Letters*, 404:296–306.

Gu, S., Liu, Z., Lynch-Stieglitz, J., Jahn, A., Zhang, J., Lindsay, K., and Wu, L. (2019). Assessing the Ability of Zonal d18O Contrast in Benthic Foraminifera to Reconstruct Deglacial Evolution of Atlantic Meridional Overturning Circulation. *Paleoceanography and Paleoclimatology*, 34(5):800–812. _eprint: https://onlinelibrary.wiley.com/doi/pdf/10.1029/2019PA003564.

Guihou, A., Pichat, S., Govin, A., Nave, S., Michel, E., Duplessy, J.-C., Telouk, P., and Labeyrie, L. (2011). Enhanced Atlantic Meridional Overturning Circulation supports the Last Glacial Inception. *Quaternary Science Reviews*, 30(13):1576–1582.

Haley, B. A., Du, J., Abbott, A. N., and McManus, J. (2017). The Impact of Benthic Processes on Rare Earth Element and Neodymium Isotope Distributions in the Oceans. *Frontiers in Marine Science*, 4:426.

Haug, G. H., Ganopolski, A., Sigman, D. M., Rosell-Mele, A., Swann, G. E. A., Tiedemann, R., Jaccard, S. L., Bollmann, J., Maslin, M. A., Leng, M. J., and Eglinton, G. (2005). North Pacific seasonality and the glaciation of North America 2.7 million years ago. *Nature*, 433(7028):821–825.

Haug, G. H., Sigman, D. M., Tiedemann, R., Pedersen, T. F., and Sarnthein, M. (1999). Onset of permanent stratification in the subarctic Pacific Ocean. *Nature*, 401(6755):779–782. Number: 6755 Publisher: Nature Publishing Group.

Hawkesworth, C., Cawood, P., Kemp, T., Storey, C., and Dhuime, B. (2009). A Matter of Preservation. *Science*, 323(5910):49–50. Publisher: American Association for the Advancement of Science.

Hay, W. W. (1996). Tectonics and climate. *Geologische Rundschau*, 85(3):409–437.

Hayashi, T., Yamanaka, T., Hikasa, Y., Sato, M., Kuwahara, Y., and Ohno, M. (2020). Latest Pliocene Northern Hemisphere glaciation amplified by intensified Atlantic meridional overturning circulation. *Communications Earth & Environment*, 1(1):25.

Haywood, A. M., Tindall, J. C., Dowsett, H. J., Dolan, A. M., Foley, K. M., Hunter, S. J., Hill, D. J., Chan, W.-L., Abe-Ouchi, A., Stepanek, C., Lohmann, G., Chandan, D., Peltier, W. R., Tan, N., Contoux, C., Ramstein, G., Li, X., Zhang, Z., Guo, C., Nisancioglu, K. H., Zhang, Q., Li, Q., Kamae, Y., Chandler, M. A., Sohl, L. E., Otto-Bliesner, B. L., Feng, R., Brady, E. C., von der Heydt, A. S., Baatsen, M. L. J., and Lunt, D. J. (2020). The Pliocene Model Intercomparison Project Phase 2: large-scale climate features and climate sensitivity. *Clim. Past*, 16(6):2095–2123. Publisher: Copernicus Publications.

Hem, J. D. (1985). *Study and interpretation of the chemical characteristics of natural water / by John D. Hem.* State Mutual Book and Periodical Service, 3rd ed edition.

Hernández-Almeida, I., Sierro, F., Cacho, I., and Flores, J.-A. (2014). Subsurface North Atlantic warming as a trigger of rapid cooling events: Evidence from the early Pleistocene (MIS 31-19). *Climate of the Past Discussions*, 10:4033–4055.

Hill, D., Haywood, A., Hindmarsh, R., and Valdes, P. (2007). Characterizing ice sheets during the Pliocene: evidence from data and models. In Williams, M., Haywood, A., Gregory, F., and Schmidt, D., editors, *Deep-Time Perspectives on Climate Change: Marrying the Signal from Computer Models and Biological Proxies*, pages 517–538. The Geological Society of London on behalf of The Micropalaeontological Society, first edition.

Hill, D. J., Bolton, K. P., and Haywood, A. M. (2017). Modelled ocean changes at the Plio-Pleistocene transition driven by Antarctic ice advance. *Nature Communications*, 8(1):14376.

Hillaire-Marcel, C., de Vernal, A., Bilodeau, G., and Weaver, A. J. (2001). Absence of deep-water formation in the Labrador Sea during the last interglacial period. *Nature*, 410(6832):1073–1077.

Hodell, D. A. and Venz, K. (1992). Toward a High-Resolution Stable Isotopic Record of the Southern Ocean During the Pliocene-Pleistocene (4.8 to 0.8 MA). In Kennett, J. P. and Warkne, D. A., editors, *Antarctic Research Series*, pages 265–310. American Geophysical Union, Washington, D. C.

Holland, K., Branson, O., Haynes, L. L., Hönisch, B., Allen, K. A., Russell, A. D., Fehrenbacher, J. S., Spero, H. J., and Eggins, S. M. (2020). Constraining multiple controls on planktic foraminifera Mg/Ca. *Geochimica et Cosmochimica Acta*, 273:116–136.

Hönisch, B., Eggins, S., Haynes, L. L., Allen, K. A., Holland, K. D., and Lorbacher, K. (2019). *Boron proxies in paleoceanography and paleoclimatology.* New analytical methods in earth and environmental science series. Wiley Blackwell, Hoboken, NJ.

Hopkins, J. L., Wysoczanski, R. J., Orpin, A. R., Howarth, J. D., Strachan, L. J., Lunenburg, R., McKeown, M., Ganguly, A., Twort, E., and Camp, S. (2020). Deposition and preservation of tephra in marine sediments at the active Hikurangi subduction margin. *Quaternary Science Reviews*, 247:106500.

Howe, J. N. W., Piotrowski, A. M., Noble, T. L., Mulitza, S., Chiessi, C. M., and Bayon, G. (2016). North Atlantic Deep Water Production during the Last Glacial Maximum. *Nature Communications*, 7(1):11765.

Hu, A. and Meehl, G. A. (2005). Bering Strait throughflow and the thermohaline circulation. *Geophysical Research Letters*, 32(24). _eprint: https://onlinelibrary.wiley.com/doi/pdf/10.1029/2005GL024424.

Hu, A., Meehl, G. A., Han, W., Abe-Ouchi, A., Morrill, C., Okazaki, Y., and Chikamoto, M. O. (2012a). The Pacific-Atlantic seesaw and the Bering Strait. *Geophysical Research Letters*, 39(3). _eprint: https://onlinelibrary.wiley.com/doi/pdf/10.1029/2011GL050567.

Hu, A., Meehl, G. A., Han, W., Timmermann, A., Otto-Bliesner, B., Liu, Z., Washington, W. M., Large, W., Abe-Ouchi, A., Kimoto, M., Lambeck, K., and Wu, B. (2012b). Role of the Bering Strait on the hysteresis of the ocean conveyor belt circulation and glacial climate stability. *Proceedings of the National Academy of Sciences*, 109(17):6417–6422. Publisher: Proceedings of the National Academy of Sciences.

Hu, A., Meehl, G. A., Otto-Bliesner, B. L., Waelbroeck, C., Han, W., Loutre, M.-F., Lambeck, K., Mitrovica, J. X., and Rosenbloom, N. (2010). Influence of Bering Strait flow and North Atlantic circulation on glacial sea-level changes. *Nature Geoscience*, 3(2):118–121.

Irving, L. (1925). THE CARBONIC ACID-CARBONATE EQUILIBRIUM AND OTHER WEAK ACIDS IN SEA WATER. *Journal of Biological Chemistry*, 63:767–778.

Jakob, K. A., Pross, J., Link, J. M., Blaser, P., Hauge Braaten, A., and Friedrich, O. (2021). Deep-ocean circulation in the North Atlantic during the Plio-Pleistocene intensification of Northern Hemisphere Glaciation (˜2.65–2.4 Ma). *Marine Micropaleontology*, 165:101998.

Jakob, K. A., Wilson, P. A., Pross, J., Ezard, T. H. G., Fiebig, J., Repschläger, J., and Friedrich, O. (2020). A new sea-level record for the Neogene/Quaternary boundary reveals transition to a more stable East Antarctic Ice Sheet. *Proceedings of the National Academy of Sciences*, 117(49):30980–30987.

Jeandel, C. (2016). Overview of the mechanisms that could explain the 'Boundary Exchange' at the land–ocean contact. *Philosophical Transactions of the Royal Society A: Mathematical, Physical and Engineering Sciences*, 374(2081):20150287.

Jeandel, C., Arsouze, T., Lacan, F., Téchiné, P., and Dutay, J.-C. (2007). Isotopic Nd compositions and concentrations of the lithogenic inputs into the ocean: A compilation, with an emphasis on the margins. *Chemical Geology*, 239(1-2):156–164.

Jellinek, A. M., Manga, M., and Saar, M. O. (2004). Did melting glaciers cause volcanic eruptions in eastern California? Probing the mechanics of dike formation. *Journal of Geophysical Research: Solid Earth*, 109(B9). _eprint: https://onlinelibrary.wiley.com/doi/pdf/10.1029/2004JB002978.

Jones, C. S. and Cessi, P. (2016). Interbasin Transport of the Meridional Overturning Circulation. *Journal of Physical Oceanography*, 46(4):1157–1169. Publisher: American Meteorological Society Section: Journal of Physical Oceanography.

Jones, C. S. and Cessi, P. (2017). Size Matters: Another Reason Why the Atlantic Is Saltier than the Pacific. *Journal of Physical Oceanography*, 47(11):2843–2859. Publisher: American Meteorological Society Section: Journal of Physical Oceanography.

Jonkers, L., Zahn, R., Thomas, A., Henderson, G., Abouchami, W., François, R., Masque, P., Hall, I. R., and Bickert, T. (2015). Deep circulation changes in the central South Atlantic during the past 145 kyrs reflected in a combined 231Pa/230Th, Neodymium isotope and benthic dC13 record. *Earth and Planetary Science Letters*, 419:14–21.

Karas, C., Nürnberg, D., Bahr, A., Groeneveld, J., Herrle, J. O., Tiedemann, R., and deMenocal, P. B. (2017). Pliocene oceanic seaways and global climate. *Scientific Reports*, 7(1):39842.

Kender, S., Bogus, K., Pedersen, G. K., Dybkjær, K., Mather, T. A., Mariani, E., Ridgwell, A., Riding, J. B., Wagner, T., Hesselbo, S. P., and Leng, M. J. (2021). Paleocene/Eocene carbon feedbacks triggered by volcanic activity. *Nature Communications*, 12(1):5186. Number: 1 Publisher: Nature Publishing Group.

Kennett, J. P. and Thunell, R. C. (1975). Global Increase in Quaternary Explosive Volcanism. *Science*, 187(4176):497–503. Publisher: American Association for the Advancement of Science.

Khélifi, N., Sarnthein, M., and Naafs, B. D. A. (2012). Technical note: Late Pliocene age control and composite depths at ODP Site 982, revisited. *Climate of the Past*, 8(1):79–87.

Kim, K.-R., Cho, Y.-K., Kang, D.-J., and Ki, J.-H. (2005). The origin of the Tsushima Current based on oxygen isotope measurement. *Geophysical Research Letters*, 32(3):L03602.

Kleiven, H. F., Jansen, E., Fronval, T., and Smith, T. M. (2002). Intensification of Northern Hemisphere glaciations in the circum Atlantic region (3.5–2.4 Ma) – ice-rafted detritus evidence. *Palaeogeography, Palaeoclimatology, Palaeoecology*, 184(3):213–223.

Kutterolf, S., Schindlbeck, J. C., Jegen, M., Freundt, A., and Straub, S. M. (2019). Milankovitch frequencies in tephra records at volcanic arcs: The relation of kyr-scale cyclic variations in volcanism to global climate changes. *Quaternary Science Reviews*, 204:1–16.

Kwiek, P. B. and Ravelo, A. C. (1999). Pacific Ocean intermediate and deep water circulation during the Pliocene. *Palaeogeography, Palaeoclimatology, Palaeoecology*, 154(3):191–217.

Lacan, F. and Jeandel, C. (2005). Neodymium isotopes as a new tool for quantifying exchange fluxes at the continent–ocean interface. *Earth and Planetary Science Letters*, 232(3):245–257.

Lacasse, C. and van den Bogaard, P. (2002). Enhanced airborne dispersal of silicic tephras during the onset of Northern Hemisphere glaciations, from 6 to 0 Ma records of explosive volcanism and climate change in the subpolar North Atlantic. *Geology*, 30(7):623.

Lambelet, M., van de Flierdt, T., Crocket, K., Rehkämper, M., Kreissig, K., Coles, B., Rijkenberg, M. J. A., Gerringa, L. J. A., de Baar, H. J. W., and Steinfeldt, R. (2016). Neodymium isotopic composition and concentration in the western North Atlantic Ocean: Results from the GEOTRACES GA02 section. *Geochimica et Cosmochimica Acta*, 177:1–29.

Lang, D. C., Bailey, I., Wilson, P. A., Chalk, T. B., Foster, G. L., and Gutjahr, M. (2016). Incursions of southern-sourced water into the deep North Atlantic during late Pliocene glacial intensification. *Nature Geoscience*, 9(5):375–379.

Larkin, C. S., Ezat, M. M., Roberts, N. L., Bauch, H. A., Spielhagen, R. F., Noormets, R., Polyak, L., Moreton, S. G., Rasmussen, T. L., Sarnthein, M., Tipper, E. T., and Piotrowski, A. M. (2022). Active Nordic Seas deep-water formation during the last glacial maximum. *Nature Geoscience*, pages 1–7. Publisher: Nature Publishing Group.

Lea, D. (2014). 8.14 - Elemental and Isotopic Proxies of Past Ocean Temperatures. In Holland, H. and Turekian, K., editors, *Treatise on Geochemistry*, pages 373–397. Elsevier Ltd, second edition edition.

Lear, C. H., Coxall, H. K., Foster, G. L., Lunt, D. J., Mawbey, E. M., Rosenthal, Y., Sosdian, S. M., Thomas, E., and Wilson, P. A. (2015). Neogene ice volume and ocean temperatures: Insights from infaunal foraminiferal Mg/Ca paleothermometry. *Paleoceanography*, 30(11):1437–1454. _eprint: https://onlinelibrary.wiley.com/doi/pdf/10.1002/2015PA002833.

Lemarchand, D., Gaillardet, J., Lewin, É., and Allègre, C. J. (2000). The influence of rivers on marine boron isotopes and implications for reconstructing past ocean pH. *Nature*, 408(6815):951–954. Number: 6815 Publisher: Nature Publishing Group.

Lemarchand, D., Gaillardet, J., Lewin, É., and Allègre, C. J. (2002). Boron isotope systematics in large rivers: implications for the marine boron budget and paleo-pH reconstruction over the Cenozoic. *Chemical Geology*, 190(1):123–140.

Lohmann, J. and Svensson, A. (2022). Ice core evidence for major volcanic eruptions at the onset of Dansgaard-Oeschger warming events. preprint, Feedback and Forcing/Ice Cores/Millenial/D-O.

Lugmair, G. and Scheinin, N. B. (1974). Sm-Nd Ages: A New Dating Method. *Meteoritics*, 19(369).

Lynch-Stieglitz, J. (2004). 6.16 Tracers of Past Ocean Circulation. In *Treatise on Geochemistry*, volume 6 of *Treatise on geochemistry*, pages 433–451. Elsevier Pergamon, Amsterdam.

Lynch-Stieglitz, J., Curry, W. B., Oppo, D. W., Ninneman, U. S., Charles, C. D., and Munson, J. (2006). Meridional overturning circulation in the South Atlantic at the last glacial maximum. *Geochemistry, Geophysics, Geosystems*, 7(10). _eprint: https://onlinelibrary.wiley.com/doi/pdf/10.1029/2005GC001226.

Maclennan, J., Jull, M., McKenzie, D., Slater, L., and Grönvold, K. (2002). The link between volcanism and deglaciation in Iceland. *Geochemistry, Geophysics, Geosystems*, 3(11):1–25. _eprint: https://agupubs.onlinelibrary.wiley.com/doi/pdf/10.1029/2001GC000282.

Marincovich, L. and Gladenkov, A. Y. (1999). Evidence for an early opening of the Bering Strait. *Nature*, 397(6715):149–151. Number: 6715 Publisher: Nature Publishing Group.

Martin, P. A., Lea, D. W., Rosenthal, Y., Shackleton, N. J., Sarnthein, M., and Papenfuss, T. (2002). Quaternary deep sea temperature histories derived from benthic foraminiferal Mg/Ca. *Earth and Planetary Science Letters*, 198(1-2):193–209.

Maslin, M. A., Haug, G. H., Sarnthein, M., and Tiedemann, R. (1996). The progressive intensification of northern hemisphere glaciation as seen from the North Pacific. *Geologische Rundschau*, 85(3):452–465.

Maslin, M. A., Haug, G. H., Sarnthein, M., Tiedemann, R., Erlenkeuser, H., and Stax, R. (1995). The Initiation of Northern Hemisphere Glaciation. In Rea, D., Basov, L., Scholl, D., and Allan, J., editors, *Proceedings of the Ocean Drilling Program, 145 Scientific Results*, volume 145 of *Proceedings of the Ocean Drilling Program*. Ocean Drilling Program.

McClymont, E. L., Ford, H. L., Ho, S. L., Tindall, J. C., Haywood, A. M., Alonso-Garcia, M., Bailey, I., Berke, M. A., Littler, K., Patterson, M. O., Petrick, B., Peterse, F., Ravelo, A. C., Risebrobakken, B., De Schepper, S., Swann, G. E. A., Thirumalai, K., Tierney, J. E., van der Weijst, C., White, S., Abe-Ouchi, A., Baatsen, M. L. J., Brady, E. C., Chan, W.-L., Chandan, D., Feng, R., Guo, C., von der Heydt, A. S., Hunter, S., Li, X., Lohmann, G., Nisancioglu, K. H., Otto-Bliesner, B. L., Peltier, W. R., Stepanek, C., and Zhang, Z. (2020). Lessons from a high-CO_2 world: an ocean view from 3 million years ago. *Climate of the Past*, 16(4):1599–1615.

McKay, R., Naish, T., Carter, L., Riesselman, C., Dunbar, R., Sjunneskog, C., Winter, D., Sangiorgi, F., Warren, C., Pagani, M., Schouten, S., Willmott, V., Levy, R., DeConto, R., and Powell, R. D. (2012). Antarctic and Southern Ocean influences on Late Pliocene global cooling. *Proceedings of the National Academy of Sciences*, 109(17):6423–6428.

McKenzie, N. R., Horton, B. K., Loomis, S. E., Stockli, D. F., Planavsky, N. J., and Lee, C.-T. A. (2016). Continental arc volcanism as the principal driver of icehouse-greenhouse variability. *Science*, 352(6284):444–447.

Menviel, L., Timmermann, A., Elison Timm, O., Mouchet, A., Abe-Ouchi, A., Chikamoto, M., Harada, N., Ohgaito, R., and Okazaki, Y. (2012). Removing the North Pacific halocline: Effects on global climate, ocean circulation and the carbon cycle. *Deep Sea Research Part II: Topical Studies in Oceanography*, 61-64:106–113.

Moffat, C., Owens, B., and Beardsley, R. C. (2009). On the characteristics of Circumpolar Deep Water intrusions to the west Antarctic Peninsula Continental Shelf. *Journal of Geophysical Research: Oceans*, 114(C5). Publisher: John Wiley & Sons, Ltd.

Molnar, P. (2008). Closing of the Central American Seaway and the Ice Age: A critical review. *Paleoceanography*, 23(2). _eprint: https://onlinelibrary.wiley.com/doi/pdf/10.1029/2007PA001574.

Naafs, B. D. A., Stein, R., Hefter, J., Khélifi, N., De Schepper, S., and Haug, G. H. (2010). Late Pliocene changes in the North Atlantic Current. *Earth and Planetary Science Letters*, 298(3):434–442.

Nakada, M. and Yokose, H. (1992). Ice age as a trigger of active Quaternary volcanism and tectonism. *Tectonophysics*, 212(3-4):321–329.

Nakayama, K. and Yoshikawa, S. (1997). Depositional processes of primary to reworked volcaniclastics on an alluvial plain; an example from the Lower Pliocene Ohta tephra bed of the Tokai Group, central Japan. *Sedimentary Geology*, 107(3):211–229.

Nürnberg, D., Ziegler, M., Karas, C., Tiedemann, R., and Schmidt, M. W. (2008). Interacting Loop Current variability and Mississippi River discharge over the past 400 kyr. *Earth and Planetary Science Letters*, 272(1-2):278–289.

Ohno, M., Hayashi, T., Komatsu, F., Murakami, F., Zhao, M., Guyodo, Y., Acton, G., Evans, H. F., and Kanamatsu, T. (2012). A detailed paleomagnetic record between 2.1 and 2.75 Ma at IODP Site U1314 in the North Atlantic: Geomagnetic excursions and the Gauss-Matuyama transition. *Geochemistry Geophysics Geosystems*, 13:Q12Z39.

Ohno, M., Hayashi, T., Sato, M., Kuwahara, Y., Mizuta, A., Kita, I., Sato, T., and Kano, A. (2016). Millennial-Scale Interaction between Ice Sheets and Ocean Circulation during Marine Isotope Stage 100. *Frontiers in Earth Science*, 4.

Ohshima, K. I., Nihashi, S., and Iwamoto, K. (2016). Global view of sea-ice production in polynyas and its linkage to dense/bottom water formation. *Geoscience Letters*, 3(1):13.

Okazaki, Y., Timmermann, A., Menviel, L., Harada, N., Abe-Ouchi, A., Chikamoto, M. O., Mouchet, A., and Asahi, H. (2010). Deepwater Formation in the North Pacific During the Last Glacial Termination. *Science*, 329(5988):200–204.

Oppo, D. W., Curry, W. B., and McManus, J. F. (2015). What do benthic d13C and d18O data tell us about Atlantic circulation during Heinrich Stadial 1? *Paleoceanography*, 30(4):353–368. _eprint: https://onlinelibrary.wiley.com/doi/pdf/10.1002/2014PA002667.

Osborne, A. H., Newkirk, D. R., Groeneveld, J., Martin, E. E., Tiedemann, R., and Frank, M. (2014). The seawater neodymium and lead isotope record of the final stages of Central American Seaway closure. *Paleoceanography*, 29(7):715–729. _eprint: https://onlinelibrary.wiley.com/doi/pdf/10.1002/2014PA002676.

Otto-Bliesner, B. L., Jahn, A., Feng, R., Brady, E. C., Hu, A., and Löfverström, M. (2017). Amplified North Atlantic warming in the late Pliocene by changes in Arctic gateways. *Geophysical Research Letters*, 44(2):957–964. _eprint: https://onlinelibrary.wiley.com/doi/pdf/10.1002/2016GL071805.

Pearson, P. N. and Palmer, M. R. (2000). Atmospheric carbon dioxide concentrations over the past 60 million years. *Nature*, 406(6797):695–699. Number: 6797 Publisher: Nature Publishing Group.

Pöppelmeier, F., Lippold, J., Blaser, P., Gutjahr, M., Frank, M., and Stocker, T. F. (2022). Neodymium isotopes as a paleo-water mass tracer: A model-data reassessment. *Quaternary Science Reviews*, 279:107404.

Praetorius, S. K., Condron, A., Mix, A. C., Walczak, M. H., McKay, J. L., and Du, J. (2020). The role of Northeast Pacific meltwater events in deglacial climate change. *Science Advances*, 6(9):eaay2915.

Prueher, L. M. and Rea, D. K. (1998). Rapid onset of glacial conditions in the subarctic North Pacific region at 2.67 Ma: Clues to causality. *Geology*, 26(11):1027.

Prueher, L. M. and Rea, D. K. (2001). Volcanic triggering of late Pliocene glaciation: evidence from the flux of volcanic glass and ice-rafted debris to the North Pacific Ocean. *Palaeogeography, Palaeoclimatology, Palaeoecology*, 173(3):215–230.

Rae, J. W., Foster, G. L., Schmidt, D. N., and Elliott, T. (2011). Boron isotopes and B/Ca in benthic foraminifera: Proxies for the deep ocean carbonate system. *Earth and Planetary Science Letters*, 302(3-4):403–413.

Rae, J. W. B., Sarnthein, M., Foster, G. L., Ridgwell, A., Grootes, P. M., and Elliott, T. (2014). Deep water formation in the North Pacific and deglacial CO_2 rise: N Pacific deep water and deglacial CO2. *Paleoceanography*, 29(6):645–667.

Rampino, M. R. and Self, S. (1993). Climate-Volcanism Feedback and the Toba Eruption of c. 74,000 Years Ago. *Quaternary Research*, 40(3):269–280.

Ravelo, A. C. and Andreasen, D. H. (2000). Enhanced circulation during a warm period. *Geophysical Research Letters*, 27(7):1001–1004.

Ravelo, A. C. and Hillaire-Marcel, C. (2007). Chapter Eighteen The Use of Oxygen and Carbon Isotopes of Foraminifera in Paleoceanography. In Hillaire-Marcel, C. and De Vernal, A., editors, *Developments in Marine Geology*, volume 1 of *Proxies in Late Cenozoic Paleoceanography*, pages 735–764. Elsevier.

Raymo, M. E. (1994). The Initiation of Northern Hemisphere Glaciation. *Annual Review of Earth and Planetary Sciences*, 22(1):353–383. Publisher: Annual Reviews.

Raymo, M. E., Grant, B., Horowitz, M., and Rau, G. H. (1996). Mid-Pliocene warmth: stronger greenhouse and stronger conveyor. *Marine Micropaleontology*, 27(1):313–326.

Raymo, M. E., Hodell, D., and Jansen, E. (1992). Response of deep ocean circulation to initiation of northern hemisphere glaciation (3-2 MA). *Paleoceanography*, 7(5):645–672.

Raymo, M. E., Kozdon, R., Evans, D., Lisiecki, L., and Ford, H. L. (2018). The accuracy of mid-Pliocene d18O-based ice volume and sea level reconstructions. *Earth-Science Reviews*, 177:291–302.

Richter, I. and Xie, S.-P. (2010). Moisture transport from the Atlantic to the Pacific basin and its response to North Atlantic cooling and global warming. *Climate Dynamics*, 35(2):551–566.

Rodríguez-Tovar, F. J., Dorador, J., and Hodell, D. A. (2019). Trace fossils evidence of a complex history of nutrient availability and oxygen conditions during Heinrich Event 1. *Global and Planetary Change*, 174:26–34.

Rosenthal, Y., Boyle, E. A., and Slowey, N. (1997). Temperature control on the incorporation of magnesium, strontium, fluorine, and cadmium into benthic foraminiferal shells from Little Bahama Bank: Prospects for thermocline paleoceanography. *Geochimica et Cosmochimica Acta*, 61(17):3633–3643.

Rosenthal, Y., Lear, C. H., Oppo, D. W., and Linsley, B. K. (2006). Temperature and carbonate ion effects on Mg/Ca and Sr/Ca ratios in benthic foraminifera: Aragonitic species *Hoeglundina elegans*: Mg AND Sr IN *HOEGLUNDINA*. *Paleoceanography*, 21(1):n/a–n/a.

Ross, C. L., DeCarlo, T. M., and McCulloch, M. T. (2019). Calibration of Sr/Ca, Li/Mg and Sr-U Paleothermometry in Branching and Foliose Corals. *Paleoceanography and Paleoclimatology*, 34(8):1271–1291. _eprint: https://onlinelibrary.wiley.com/doi/pdf/10.1029/2018PA003426.

Ruddiman, W., Kidd, R., Thomas, E., and et al. (1987). *Initial Reports of the Deep Sea Drilling Project, 94*, volume 94 of *Initial Reports of the Deep Sea Drilling Project*. U.S. Government Printing Office.

Schindlbeck, J. C., Kutterolf, S., Freundt, A., Eisele, S., Wang, K., and Frische, M. (2018). Miocene to Holocene Marine Tephrostratigraphy Offshore Northern Central America and Southern Mexico: Pulsed Activity of Known Volcanic Complexes. *Geochemistry, Geophysics, Geosystems*, 19(11):4143–4173.

Schlitzer, R. (2000). Electronic Atlas of WOCE Hydrographic and Tracer Data Now Available. *Eos Trans*, 81(5):45.

Schmidt, M. W., Spero, H. J., and Lea, D. W. (2004). Links between salinity variation in the Caribbean and North Atlantic thermohaline circulation. *Nature*, 428(6979):160–163.

Schmidt, P., Lund, B., Hieronymus, C., Maclennan, J., Árnadóttir, T., and Pagli, C. (2013). Effects of present-day deglaciation in Iceland on mantle melt production rates. *Journal of Geophysical Research: Solid Earth*, 118(7):3366–3379. _eprint: https://onlinelibrary.wiley.com/doi/pdf/10.1002/jgrb.50273.

Schmitt, A., Elliot, M., Thirumalai, K., La, C., Bassinot, F., Petersen, J., Movellan, A., Jorry, S. J., and Borgomano, J. (2019). Single foraminifera Mg/Ca analyses of past glacial-interglacial temperatures derived from G. ruber sensu stricto and sensu lato morphotypes. *Chemical Geology*, 511:510–520.

Schmittner, A., Bostock, H. C., Cartapanis, O., Curry, W. B., Filipsson, H. L., Galbraith, E. D., Gottschalk, J., Herguera, J. C., Hoogakker, B., Jaccard, S. L., Lisiecki, L. E., Lund, D. C., Martínez-Méndez, G., Lynch-Stieglitz, J., Mackensen, A., Michel, E., Mix, A. C., Oppo, D. W., Peterson, C. D., Repschläger, J., Sikes, E. L., Spero, H. J., and Waelbroeck, C. (2017). Calibration of the carbon isotope composition (d13C) of benthic foraminifera. *Paleoceanography*, 32(6):512–530. _eprint: https://onlinelibrary.wiley.com/doi/pdf/10.1002/2016PA003072.

Sepulchre, P., Arsouze, T., Donnadieu, Y., Dutay, J.-C., Jaramillo, C., Le Bras, J., Martin, E., Montes, C., and Waite, A. J. (2014). Consequences of shoaling of the Central American Seaway determined from modeling Nd isotopes. *Paleoceanography*, 29(3):176–189. _eprint: https://onlinelibrary.wiley.com/doi/pdf/10.1002/2013PA002501.

Shackleton, N. J. (1987). Oxygen isotopes, ice volume and sea level. *Quaternary Science Reviews*, 6(3):183–190.

Shankle, M. G., Burls, N. J., Fedorov, A. V., Thomas, M. D., Liu, W., Penman, D. E., Ford, H. L., Jacobs, P. H., Planavsky, N. J., and Hull, P. M. (2021). Pliocene decoupling of equatorial Pacific temperature and pH gradients. *Nature*, 598(7881):457–461.

Sigl, M., Winstrup, M., McConnell, J. R., Welten, K. C., Plunkett, G., Ludlow, F., Büntgen, U., Caffee, M., Chellman, N., Dahl-Jensen, D., Fischer, H., Kipfstuhl, S., Kostick, C., Maselli, O. J., Mekhaldi, F., Mulvaney, R., Muscheler, R., Pasteris, D. R., Pilcher, J. R., Salzer, M., Schüpbach, S., Steffensen, J. P., Vinther, B. M., and Woodruff, T. E. (2015). Timing and climate forcing of volcanic eruptions for the past 2,500 years. *Nature*, 523(7562):543–549. Number: 7562 Publisher: Nature Publishing Group.

Sigman, D. M. and Boyle, E. A. (2000). Glacial/interglacial variations in atmospheric carbon dioxide. *Nature*, 407(6806):859–869.

Sigman, D. M., Hain, M. P., and Haug, G. H. (2010). The polar ocean and glacial cycles in atmospheric CO2 concentration. *Nature*, 466(7302):47–55.

Sigman, D. M., Jaccard, S. L., and Haug, G. H. (2004). Polar ocean stratification in a cold climate. *Nature*, 428(6978):59–63.

Sigmundsson, F., Albino, F., Schmidt, P., Lund, B., Pinel, V., Hooper, A., and Pagli, C. (2012). Multiple Effects of Ice Load Changes and Associated Stress Change on Magmatic Systems. In McGuire, B. and Maslin, M., editors, *Climate Forcing of Geological Hazards*, pages 108–123. John Wiley & Sons, Ltd, Chichester, UK.

Sigmundsson, F., Pinel, V., Lund, B., Albino, F., Pagli, C., Geirsson, H., and Sturkell, E. (2010). Climate effects on volcanism: influence on magmatic systems of loading and unloading from ice mass variations, with examples from Iceland. *Philosophical Transactions of the Royal Society A: Mathematical, Physical and Engineering Sciences*, 368(1919):2519–2534.

Skinner, L. C., Freeman, E., Hodell, D., Waelbroeck, C., Riveiros, N. V., and Scrivner, A. (2020). Atlantic Ocean ventilation changes across the last deglaciation and their carbon cycle implications. *Paleoceanography and Paleoclimatology*.

Sosdian, S. and Rosenthal, Y. (2009). Deep-Sea Temperature and Ice Volume Changes Across the Pliocene-Pleistocene Climate Transitions. *Science*, 325(5938):306–310.

Sosdian, S. and Rosenthal, Y. (2010). Response to Comment on "Deep-Sea Temperature and Ice Volume Changes Across the Pliocene-Pleistocene Climate Transitions". *Science*, 328(5985):1480–1480. Publisher: American Association for the Advancement of Science.

Steinke, S., Chiu, H.-Y., Yu, P.-S., Shen, C.-C., Löwemark, L., Mii, H.-S., and Chen, M.-T. (2005). Mg/Ca ratios of two Globigerinoides ruber (white) morphotypes: Implications for reconstructing past tropical/subtropical surface water conditions. *Geochemistry, Geophysics, Geosystems*, 6(11). _eprint: https://onlinelibrary.wiley.com/doi/pdf/10.1029/2005GC000926.

Stirpe, C. R., Allen, K. A., Sikes, E. L., Zhou, X., Rosenthal, Y., Cruz-Uribe, A. M., and Brooks, H. L. (2021). The Mg/Ca proxy for temperature: A Uvigerina core-top study in the Southwest Pacific. *Geochimica et Cosmochimica Acta*, 309:299–312.

Stocker, T. F. and Wright, D. G. (1991). Rapid transitions of the ocean's deep circulation induced by changes in surface water fluxes. *Nature*, 351(6329):729–732. Number: 6329 Publisher: Nature Publishing Group.

Stow, D., Hunter, S., Wilkinson, D., and Hernández-Molina, F. (2008). Chapter 9 The Nature of Contourite Deposition. In Rebesco, M. and Camerlenghi, A., editors, *Developments in Sedimentology*, volume 60, pages 143–156. Elsevier.

Struve, T., Wilson, D. J., Hines, S. K. V., Adkins, J. F., and van de Flierdt, T. (2022). A deep Tasman outflow of Pacific waters during the last glacial period. *Nature Communications*, 13(1):3763. Number: 1 Publisher: Nature Publishing Group.

Studer, A. S., Martínez-Garcia, A., Jaccard, S. L., Girault, F. E., Sigman, D. M., and Haug, G. H. (2012). Enhanced stratification and seasonality in the Subarctic Pacific upon Northern Hemisphere Glaciation–New evidence from diatom-bound nitrogen isotopes, alkenones and archaeal tetraethers. *Earth and Planetary Science Letters*, 351-352:84–94.

Swann, G. E. (2010). Salinity changes in the North West Pacific Ocean during the late Pliocene/early Quaternary from 2.73Ma to 2.52Ma. *Earth and Planetary Science Letters*, 297(1-2):332–338.

Swann, G. E. A., Maslin, M. A., Leng, M. J., Sloane, H. J., and Haug, G. H. (2006). Diatom d18O evidence for the development of the modern halocline system in the subarctic northwest Pacific at the onset of major Northern Hemisphere glaciation. *Paleoceanography*, 21(1). _eprint: https://onlinelibrary.wiley.com/doi/pdf/10.1029/2005PA001147.

Tachikawa, K., Jeandel, C., and Roy-Barman, M. (1999). A new approach to the Nd residence time in the ocean: the role of atmospheric inputs. *Earth and Planetary Science Letters*, 170(4):433–446.

Tachikawa, K., Piotrowski, A. M., and Bayon, G. (2014). Neodymium associated with foraminiferal carbonate as a recorder of seawater isotopic signatures. *Quaternary Science Reviews*, 88:1–13.

Talley, L. (2013). Closure of the Global Overturning Circulation Through the Indian, Pacific, and Southern Oceans: Schematics and Transports. *Oceanography*, 26(1):80–97.

Talley, L. D. (1993). Distribution and Formation of North Pacific Intermediate Water. *Journal of Physical Oceanography*, 23(3):517–537.

Talley, L. D., Pickard, G. L., Emery, W. J., and Swift, J. H. (2011). Chapter 9 - Atlantic Ocean. In Talley, L. D., Pickard, G. L., Emery, W. J., and Swift, J. H., editors, *Descriptive Physical Oceanography (Sixth Edition)*, pages 245–301. Academic Press, Boston.

Tan, N., Contoux, C., Ramstein, G., Sun, Y., Dumas, C., Sepulchre, P., and Guo, Z. (2020). Modeling a modern-like pCO2 warm period (Marine Isotope Stage KM5c) with two versions of an Institut Pierre Simon Laplace atmosphere–ocean coupled general circulation model. *Clim. Past*, 16(1):1–16. Publisher: Copernicus Publications.

Thirumalai, K., Quinn, T. M., and Marino, G. (2016). Constraining past seawater d^{18} O and temperature records developed from foraminiferal geochemistry. *Paleoceanography*, 31(10):1409–1422.

Thomas, M. D., Fedorov, A. V., Burls, N. J., and Liu, W. (2021). Oceanic Pathways of an Active Pacific Meridional Overturning Circulation (PMOC). *Geophysical Research Letters*, 48(10).

Toggweiler, J. R. and Samuels, B. (1995). Effect of Sea Ice on the Salinity of Antarctic Bottom Waters. *Journal of Physical Oceanography*, 25(9):1980–1997. Place: Boston MA, USA Publisher: American Meteorological Society.

Tripati, A. K., Roberts, C. D., and Eagle, R. A. (2009). Coupling of CO2 and Ice Sheet Stability over Major Climate Transitions of the Last 20 Million Years. *Science (American Association for the Advancement of Science)*, 326(5958):1394–1397. Place: Washington, DC Publisher: Washington, DC: American Association for the Advancement of Science.

Uchikawa, J., Harper, D. T., Penman, D. E., Zachos, J. C., and Zeebe, R. E. (2017). Influence of solution chemistry on the boron content in inorganic calcite grown in artificial seawater. *Geochimica et Cosmochimica Acta*, 218:291–307.

Uchikawa, J., Penman, D. E., Zachos, J. C., and Zeebe, R. E. (2015). Experimental evidence for kinetic effects on B/Ca in synthetic calcite: Implications for potential B(OH)4 and B(OH)3 incorporation. *Geochimica et Cosmochimica Acta*, 150:171–191.

van de Flierdt, T., Griffiths, A. M., Lambelet, M., Little, S. H., Stichel, T., and Wilson, D. J. (2016). Neodymium in the oceans: a global database, a regional comparison and implications for palaeoceanographic research. *Philosophical Transactions of the Royal Society A: Mathematical, Physical and Engineering Sciences*, 374(2081):20150293.

van de Flierdt, T., Robinson, L. F., Adkins, J. F., Hemming, S. R., and Goldstein, S. L. (2006). Temporal stability of the neodymium isotope signature of the Holocene to glacial North Atlantic. *Paleoceanography*, 21(4). _eprint: https://onlinelibrary.wiley.com/doi/pdf/10.1029/2006PA001294.

van der Weijst, C. M. H., Winkelhorst, J., Lourens, L., Raymo, M. E., Sangiorgi, F., and Sluijs, A. (2020). A Ternary Mixing Model Approach Using Benthic Foraminifer d^{13}C - d^{18}O Data to Reconstruct Late Pliocene Deep Atlantic Water Mass Mixing. *Paleoceanography and Paleoclimatology*, 35(12).

Venti, N. L., Billups, K., and Herbert, T. D. (2017). Paleoproductivity in the northwestern Pacific Ocean during the Pliocene-Pleistocene climate transition (3.0–1.8 Ma). *Paleoceanography*, 32(2):92–103.

Warren, B. A. (1983). Why is no deep water formed in the North Pacific? *Journal of Marine Research*, 41:327–347.

Wastegård, S., Björck, S., Possnert, G., and Wohlfarth, B. (1998). Evidence for the occurrence of Vedde Ash in Sweden: radiocarbon and calendar age estimates. *Journal of Quaternary Science*, 13(3):271–274. _eprint: https://onlinelibrary.wiley.com/doi/pdf/10.1002/%28SICI%291099-1417%28199805/06%2913%3A3%3C271%3A%3AAID-JQS372%3E3.0.CO%3B2-4.

Watt, S. F. L., Pyle, D. M., and Mather, T. A. (2013). The volcanic response to deglaciation: Evidence from glaciated arcs and a reassessment of global eruption records. *Earth-Science Reviews*, 122:77–102.

Weiffenbach, J. E., Baatsen, M. L. J., Dijkstra, H. A., von der Heydt, A. S., Abe-Ouchi, A., Brady, E. C., Chan, W.-L., Chandan, D., Chandler, M. A., Contoux, C., Feng, R., Guo, C., Han, Z., Haywood, A. M., Li, Q., Li, X., Lohmann, G., Lunt, D. J., Nisancioglu, K. H., Otto-Bliesner, B. L., Peltier, W. R., Ramstein, G., Sohl, L. E., Stepanek, C., Tan, N., Tindall, J. C., Williams, C. J. R., Zhang, Q., and Zhang, Z. (2022). Unraveling the mechanisms and implications of a stronger mid-Pliocene AMOC in PlioMIP2. *Clim. Past Discuss.*, 2022:1–34. Publisher: Copernicus Publications.

Weldeab, S., Schneider, R. R., and Kölling, M. (2006). Comparison of foraminiferal cleaning procedures for Mg/Ca paleothermometry on core material deposited under varying terrigenous-input and bottom water conditions. *Geochemistry, Geophysics, Geosystems*, 7(4). _eprint: https://onlinelibrary.wiley.com/doi/pdf/10.1029/2005GC000990.

Wilkens, R. H., Westerhold, T., Drury, A. J., Lyle, M., Gorgas, T., and Tian, J. (2017). Revisiting the Ceara Rise, equatorial Atlantic Ocean: isotope stratigraphy of ODP Leg 154 from 0 to 5 Ma. *Climate of the Past*, 13(7):779–793.

Wilson, K. (2011). *Plio-Pleistocene reconstruction of East African and Arabian Sea palaeoclimate.* Ph.D. Thesis, University College London, Department of Geography.

Winnick, M. J. and Caves, J. K. (2015). Oxygen isotope mass-balance constraints on Pliocene sea level and East Antarctic Ice Sheet stability. *Geology*, 43(10):879–882.

Woodard, S. C., Rosenthal, Y., Miller, K. G., Wright, J. D., Chiu, B. K., and Lawrence, K. T. (2014). Antarctic role in Northern Hemisphere glaciation. *Science*, 346(6211):847–851.

Xu, X., Bower, A., Furey, H., and Chassignet, E. P. (2018). Variability of the Iceland-Scotland Overflow Water Transport Through the Charlie-Gibbs Fracture Zone: Results From an Eddying Simulation and Observations. *Journal of Geophysical Research: Oceans*, 123(8):5808–5823.

Yin, S., Hernández-Molina, F. J., Jutzeler, M., and Li, J. (2022). Progressive intensification of Pacific Deep Water circulation since the early Pliocene. *Geophysical Research Letters*.

You, Y. (2003). The pathway and circulation of North Pacific Intermediate Water: THE PATHWAY AND CIRCULATION OF NPIW. *Geophysical Research Letters*, 30(24).

Yu, J., Anderson, R. F., and Rohling, E. J. (2014). Deep Ocean Carbonate Chemistry and Glacial-Interglacial Atmospheric CO2 Changes. *Oceanography*, 27(1):16–25. Publisher: Oceanography Society.

Yu, J. and Broecker, W. S. (2010). Comment on "Deep-Sea Temperature and Ice Volume Changes Across the Pliocene-Pleistocene Climate Transitions". *Science*, 328(5985):1480–1480. Publisher: American Association for the Advancement of Science.

Yu, J. and Elderfield, H. (2007). Benthic foraminiferal B/Ca ratios reflect deep water carbonate saturation state. *Earth and Planetary Science Letters*, 258(1-2):73–86.

Yu, J. and Elderfield, H. (2008). Mg/Ca in the benthic foraminifera Cibicidoides wuellerstorfi and Cibicidoides mundulus: Temperature versus carbonate ion saturation. *Earth and Planetary Science Letters*, 276(1-2):129–139.

Yu, J., Elderfield, H., Greaves, M., and Day, J. (2007). Preferential dissolution of benthic foraminiferal calcite during laboratory reductive cleaning. *Geochemistry, Geophysics, Geosystems*, 8(6). _eprint: https://onlinelibrary.wiley.com/doi/pdf/10.1029/2006GC001571.

Yu, J., Elderfield, H., and Piotrowski, A. M. (2008). Seawater carbonate ion-d13C systematics and application to glacial–interglacial North Atlantic ocean circulation. *Earth and Planetary Science Letters*, 271(1):209–220.

Zhang, Z., Li, X., Guo, C., Otterå, O. H., Nisancioglu, K. H., Tan, N., Contoux, C., Ramstein, G., Feng, R., Otto-Bliesner, B. L., Brady, E., Chandan, D., Peltier, W. R., Baatsen, M. L. J., von der Heydt, A. S., Weiffenbach, J. E., Stepanek, C., Lohmann, G., Zhang, Q., Li, Q., Chandler, M. A., Sohl, L. E., Haywood, A. M., Hunter, S. J., Tindall, J. C., Williams, C., Lunt, D. J., Chan, W.-L., and Abe-Ouchi, A. (2021). Mid-Pliocene Atlantic Meridional Overturning Circulation simulated in PlioMIP2. *Climate of the Past*, 17(1):529–543. Publisher: Copernicus GmbH.

Zhang, Z.-S., Nisancioglu, K. H., Chandler, M. A., Haywood, A. M., Otto-Bliesner, B. L., Ramstein, G., Stepanek, C., Abe-Ouchi, A., Chan, W.-L., Bragg, F. J., Contoux, C., Dolan, A. M., Hill, D. J., Jost, A., Kamae, Y., Lohmann, G., Lunt, D. J., Rosenbloom, N. A., Sohl, L. E., and Ueda, H. (2013). Mid-pliocene Atlantic Meridional Overturning Circulation not unlike modern. *Climate of the Past*, 9(4):1495–1504. Publisher: Copernicus GmbH.

Zhu, Y., Toon, O. B., Jensen, E. J., Bardeen, C. G., Mills, M. J., Tolbert, M. A., Yu, P., and Woods, S. (2020). Persisting volcanic ash particles impact stratospheric SO2 lifetime and aerosol optical properties. *Nature Communications*, 11(1):4526. Number: 1 Publisher: Nature Publishing Group.